Experimental investigation of CFS to Steel connection using self-drilling screws

Anu Antony

A thesis submitted in fulfillment of the requirements for the degree of

Master of Engineering

Main supervisor: Dr Zhiyuan (Arthur) Fang

Co-supervisor: Prof James Lim, Dr Kris Roy

School of Engineering

The University of Waikato

New Zealand

THE UNIVERSITY OF
WAIKATO
Te Whare Wānanga o Waikato

2025

Abstract:

Screws are one of the most used methods for joining structural steel to Cold Formed Steel (CFS). An improved substitute for conventional nail and bolt connections is self-drilling screws. The wings in the screws make it easier to drive the screw into the steel without the use of a pre-drilled hole. Given that joints are the primary means of transferring energy to a structure, it is especially crucial to comprehend the seismic behaviour of their connection. New Zealand, for example, is a country that primarily experiences seismic activity and builds its buildings using a combination of structural steel and CFS. Numerous research that looks into how structural joints behave under cyclic and monotonic loading conditions are available in the literature. However, the majority of these studies did not address the use of self-drilling screws in cyclic stress to link CFS to structural steel. Thus, by experimental testing, this research examines the load deformation and failure mechanisms of CFS and steel connections utilising screws under cyclic and monotonic loads.

Tensile testing was done to evaluate the material's properties of steel. A total of 54 experimental investigations were conducted to determine the cyclic nature of the junction. The structural steel thickness (8mm, 12mm, 16mm, and 20mm), the CFS thickness (1.8mm), and the screw diameter (6.3mm hexagonal screw), and varying the number of screws (1 and 2) were considered in test program. The same samples were subjected to monotonic tests in order to determine the maximum and minimum displacement for the cyclic loading. A total of 24 tests were performed in order to acquire the values. The experiment's findings, including load deformation and the failure process, are identified. Based on the contrasting data, the cyclic nature of all the connections can be analysed to ascertain which is the most correct.

The New Zealand standard AS/NZS 4600:2018, which particularly addresses the screw spacing with each other and the distance from the screw to the edge of the specimen, will serve as the basis for both the assembly and the spacing of the structural joints. The loading procedures and the number of cycles employed for cyclic loading are detailed in the Federal Emergency Management Agency 461 (FEMA). Appropriate displacement amplitudes for cyclic tests were determined using the initial results from the

monotonic tests.

During the cyclic testing it could be found that most of the specimens failed due to bearing and tear out failure. There is an average increase of 56.77 % in capacity as the number of screws were increased from single screw to double screw connection. As the steel thickness was increased as 8mm, 12mm, 16mm, and 20mm, the average capacity was reduced to 10.13%, 18.11%, 7.98% accordingly for a single screw connection. For double screw connection as the steel thickness was increased as 8mm,12mm, 16mm, and 20mm, the average capacity was increased to 0.79%, 4.91%, 2.15% accordingly.

Key words: Self-drilling screw, Cold Formed Steel (CFS), Structural steel, Cyclic loading, Monotonic loading, Load deformation, Failure mechanisms, Tensile testing, Screw spacing, Federal Emergency Management Agency (FEMA) 461, Bearing and tear-out failure, Steel thickness, Displacement amplitudes.

Contents

List of Figures

List of Tables

Outline of the thesis

This thesis consists of eleven chapters:

- Introduction – chapter 1 methods used and the objectives of the study.
- Literature review – chapter 2 presents the background of steel-CFS structural evaluation of connection
- Material Tests - chapter 3 describes the physical properties of the materials used in this study delivered from the performed material properties tests.
- Specimen description and testing arrangement - chapter 4 provides the specimen construction, testing arrangements and instrumentation for testing
- Specimen loading – chapter 5 provides the details about loading protocols for monotonic and cyclic testing
- Fastener load-deformation monotonic and cyclic response – chapter 6 discusses the backbone nomenclature, construction and procedure for monotonic and cyclic response
- Monotonic test results – chapter 7 provides the monotonic test results about screw parameters, steel thickness and load displacement relationship
- Cyclic test results – chapter 8 provides the cyclic test results about screw parameters, and steel thickness
- Conclusions and future study - chapter 9 provides conclusion of the current study and limitations in the research.
- Acknowledgment – chapter 10.
- References – chapter 11.
- Appendix A. Monotonic test for single screw connection, Appendix B. Monotonic test for double screw connection, Appendix C. Cyclic test for single screw connection, Appendix D. Cyclic test for double screw connection,

1. Introduction

Modern construction has found favour with cold-formed steel (CFS) because of its advantageous qualities, which include a high strength-to-weight ratio, ease of manufacture, and adaptability. In contrast to conventional hot-rolled steel, CFS is produced by pressing or rolling steel into thin sheets at room temperature, which makes the material more pliable and lighter. Because of this feature, CFS is perfect for use in both load-bearing applications like roof trusses and floor joists as well as non-load-bearing elements like partition walls. Ensuring dependable and effective connections between CFS members and between CFS and other structural elements, including structural steel, is a critical component of using CFS in construction. The performance of these connections, particularly when dynamic stresses like those brought on by wind or seismic activity are present. Self-drilling screws (SDS) as shown in Figure (1) have become a popular choice among connection methods because they are inexpensive, easy to install, and make strong, long-lasting connections. The application of SDS can be seen throughout the construction industry, for instance in built-up steel structures to enhance stability (Fang et al. 2022a, b, c), in joint connections (Roy et al. 2021; Roy et al. 2022a, b; Roy et al. 2023; Feng et al. 2020), and in hybrid construction (Ng et al. 2023). SDSs are especially useful in these connections since they allow for speedy assembly and do not require pre-drilled holes, which saves money on labour and materials. One of the primary problems in this type of construction is how the joints will behave when subjected to seismic waves. Joints are the main parts of a building that are in charge of distributing energy. Among many other types of connections, the screw connection is one of the most commonly used. It is essential to comprehend how CFS behaves in relation to structural steel connections under cyclic loading. Cyclic testing replicates the effects of recurrent or varying loads, simulating natural events like as strong winds and earthquakes. This kind of testing aids in assessing the connections' long-term performance and robustness.

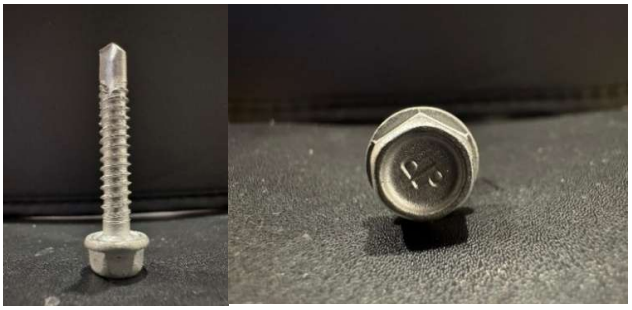

Figure 1 Hexagonal head Self-drilling Screw

Using SDS, monotonic loading experiments on CFS to structural steel connections are used to determine key performance characteristics such as ultimate load capacity, stiffness, and ductility. These tests provide crucial information on how the connections respond to steady and gradually increasing loads by simulating circumstances that are comparable to the gradual buildup of load in structural applications. These tests' load-distortion characteristics demonstrate how robust and strong the connection is to loads without suffering noticeably from deformation or failure. Understanding these characteristics is essential for creating safe and reliable systems because it ensures that the connections can support expected service loads and provides a basis for forecasting how they will behave in complex loading situations, such as cyclic or variable loads. All things considered, self-drilling screws offer a dependable and practical alternative for CFS to structural steel connections, and their structural performance must be confirmed with monotonic loading testing.

During low-cycle testing Figure (2), steel-steel connections are loaded through a predetermined number of loading cycles at relatively high loads, often until failure occurs. Understanding the fatigue resistance, failure mechanisms, and cyclic behaviour of steel-steel connections under realistic loading scenarios such as those that arise from seismic occurrences or repetitive stress in structural systems is the aim of these investigations. Through experimental testing, researchers like Tao et al. (2016) and Danquah et al. (2021) examine characteristics such as displacement, load, and deformation response. These tests allow them to assess factors including energy dissipation, the beginning of plastic deformation, and stiffness degradation. Low-cycle testing yields important information that can be utilised to enhance steel

connection performance and design by verifying that steel connections in structures can withstand cyclic stress for the length of their intended lifespan without experiencing early failure or deterioration.

Figure 2 Specimen Arrangement

2. Literature Review

2.1 CFS- Structural steel under Cyclic Loading

Tao et al. (2016) explore both the monotonic and cyclic responses of single shear cold-formed steel (CFS) connections—specifically CFS-to-steel and sheathing-to-steel connections. Each combination was subjected to both monotonic and cyclic loading with three trials each, totalling 222 tests. These connections are frequently found in light-framed buildings, and the study provides detailed insights into their load-deformation behaviour. Key variables such as steel ply thickness, fastener types, and sheathing materials are highlighted for their significant impact on the connections' strength and stiffness. Abaszadeh et al. (2021) further investigate the performance of CFS frames under cyclic loading using finite element model, particularly in the context of seismic resilience. This research is vital for assessing how CFS connections hold up under dynamic conditions, such as earthquakes. The study's findings emphasise the importance of connection design in improving seismic performance and ensuring structural integrity. By understanding the behaviour of these connections under cyclic loads, engineers can refine design practices and create more resilient CFS structures. The results offer critical data for guiding the design and construction of CFS frames, particularly in seismic regions.

2.2 CFS-structural steel under static loading

Chung et al. (2000) investigates the behaviour of bolted connections between cold formed steel strips and hot rolled steel plates when subjected to static shear loading. It aims to develop and validate a finite element (FE) model to accurately simulate these connections. The FE model provides a detailed understanding of the connection behaviour, including stress distribution and load carrying capacity. The validated FE model is effective for predicting the performance of bolted connections under static shear loads ad can be used for design and analysis purposes. Calderoni et al. (2009) investigates the behaviour of cold formed steel beams in monotonic loading. Experimental tests were conducted to evaluate the response of CFS beam subjected to static, monotonic loading. The study aims to understand their strength, stiffness and failure modes. The result provides insight into the load carrying capacity and deformation characteristics of CFS beam. Tao et al. (2016) conducted 222 tests aiming to evaluate the behaviour of single shear connections involving cold formed steel and shear thing to steel connections in monotonic loading conditions. The focus here is on understanding their performance under monotonic loads. The findings provide insight into the performance of CFS connections under monotonic loading conditions, including their load carrying capacity and deformation behaviour.

2.3 Structural Steel-Structural steel under cyclic loading

Danquah et al. (2021) present an experimental study on light-gauge steel screw and powder-actuated fastener joints under monotonic and cyclic loads, determining backbone parameters for the pinching hysteretic model, unloading-reloading characteristics, and highlighting the significant influence of loading rates on joint responses. Similarly, Beutel et al. (2002) explore the cyclic behaviour of concrete-filled steel tubular (CFST) column-to-steel beam connections, emphasizing the stability and high ductility of these connections for non-seismic applications but cautioning against designing for yield at the column face in seismic conditions due to potential local damage, underlining the importance of conservative design and adequate bar anchorage. Calderoni et al. (2009) and Kishiki et al. (2019) both examined cyclic loading in steel structures, with Calderoni identifying significant strength and stiffness degradation alongside energy dissipation potential in cold-formed steel beams, and Kishiki focusing on low-cycle

fatigue in Japanese steel beam-to-column connections, offering an empirical method for evaluating fatigue based on beam rotation amplitude and cycles to failure, highlighting the influence of slip behaviour and out-of-plane deformation on connection fatigue performance. Mroziński et al. (2019) also studied low-cycle fatigue, specifically in P91 steel, revealing cyclic softening and the role of testing conditions on fatigue life predictions, which complements Macillo et al.'s (2014) comparison of seismic design criteria in American and European codes for strap-braced cold-formed steel systems, emphasizing the conservatism of European provisions and their potential impact on improving seismic performance. This theme of cyclic performance under dynamic loading is echoed by Li et al. (2022), who demonstrated that demountable reinforced concrete (RC) column-to-steel beam connections exhibit higher lateral capacity and better energy absorption compared to non-detachable joints, providing insights for more resilient connection designs. Mashaly et al. (2011) added to this with a 3D finite element model predicting the behavior of steel beam-to-column joints under lateral loads, proposing improvements in bolt modeling and contact elements based on validated experimental data. Studies by Ballio et al. (1997) and Popov et al. (1972) further contribute to the understanding of steel members and connections under low-cycle fatigue, particularly in seismic regions, offering valuable insights into how repeated dynamic loading affects durability and design requirements. He et al. (2010) and Calado et al. (2000) extended this focus by investigating steel beam-to-column joints and semi-rigid connections, respectively, under dynamic loading, providing experimental and numerical data that support better design practices for seismic applications. Finally, Mander et al. (1994) explored low-cycle fatigue in reinforcing steel, offering critical insights into material degradation under repeated loading and its implications for the seismic resilience of reinforced concrete structures, thus contributing to a broader understanding of how both steel and concrete connections perform under the stress of dynamic events like earthquakes.

2.4 Structural Steel-Structural steel under static loading

Danquah et al. (2021) investigates the behaviour of single shear connections using steel to steel screw and powder actuated fasteners under monotonic loading conditions. The focus here is on understanding the performance of these connections. The results reveals the load carrying capacity and deformation

characteristics of the connections when subjected to monotonic shear loading. The findings contribute to the design and evaluation of connections using screws and powder actuated fasteners, particularly in static loading scenarios. Beutel et al. (2001) investigate the monotonic behaviour of composite column to beam connections, specifically analysing how these connections perform under static, monotonic loading conditions. The research aims to provide insight into the street strength, stiffness, and failure mechanisms. The results reveal key aspects of the load carrying capacity and deformation characteristics of composite column to beam connections under monotonic loading. Deng et al. (2018) investigate the monotonic behaviour of bolted connections that include a welded cover plate, specifically designed for modular steel construction. The focus here is on understanding the performance of these connections under monotonic loading conditions. The findings contribute to the design and optimization of bolted connections with welded cover plates in modular steel construction, ensuring they meet static load requirements effectively. Cao et al. (2021) investigate the behaviour if bolted connections under monotonic loading, with the aim of developing an analytical model to predict their performance accurately. They combine experimental testing with analytical modeling to enhance the understanding of these connections. The findings contribute to the development of reliable design tools and guidelines for bolted connections under static loading conditions.

2.5 Steel-timber under cyclic loading

Bellini et al. (2020) conducted an experimental study on enhancing the load-bearing capacity and stiffness of steel-to-CLT panel nailed joints using composite reinforcement, finding that reinforcement significantly improved capacity and stiffness, leading to reduced displacements, and validating a simplified design procedure for reinforced connections that aligns with experimental results. Similarly, Fiorino et al. (2007) explored screw connections between wood- or gypsum-based panels and cold-formed steel stud profiles, proposing a method to predict the lateral load-displacement response of steel frame/panel systems based on cyclic tests of different panel types, orientations, and loading rates. Ataei et al. (2018) further investigated the cyclic behavior of steel-timber composite (STC) connections, showed that these connections exhibited high ductility and energy dissipation under large slips without significant

strength loss, making them suitable for earthquake-resistant designs. An analytical hysteretic model was calibrated in OPENSEES software to predict the cyclic behavior of these connections accurately. Izzi et al. (2018) and Gavric et al. (2014) also contributed to understanding seismic performance, with Izzi praising CLT structures for their strength-to-weight ratio and ductile connections, providing recommendations for experimental testing and design, while Gavric emphasized capacity-based design principles to improve the seismic resistance of metal connectors in CLT structures. Izzi et al. (2019) further explored low-cycle ductile performance, noting that self-tapping screws of 8mm and 10mm diameters showed better potential for higher ductility classes than 6mm screws, with production processes influencing performance. Latour et al. (2015) focused on specialized dissipative connectors for CLT panel buildings, demonstrating through experimental and numerical studies that these connectors effectively absorbed and dissipated energy during cyclic loads, enhancing seismic performance, and offering a reliable modeling approach for their integration into CLT panel systems. These studies collectively contribute to the growing body of knowledge on improving the seismic resilience and performance of timber and hybrid steel-timber connections, emphasizing the importance of ductility, energy dissipation, and capacity-based design in enhancing structural safety under dynamic loading conditions.

2.6 Steel-timber under static loading

Hossain et al. (2018) investigated the performance of CLT panels connected with self-tapping screws (STS) under shear, withdrawal, and combined loading conditions. The findings revealed that shear-loaded connections offer high ductility but low stiffness, whereas withdrawal-loaded connections are very stiff but brittle. The study emphasized the importance of combining STS in both shear and withdrawal to achieve connections with high stiffness and ductility in CLT structures. Similarly, Vella et al. (2020) examined the performance of connections between cold-formed steel (CFS) and timber using inclined screws, which is crucial for understanding how such connections behave under various loading conditions in mixed-material construction. Their study focused on evaluating the strength, stiffness, and effectiveness of these connections, particularly for structural design applications. Ying Ng et al. (2023) also explored the performance of timber-to-CFS connections using self-drilling screws, providing valuable insights into

their behavior under different loading conditions, which is critical for designing effective and reliable mixed-material structures. Chen et al. (2021) added to this understanding by investigating the performance of thin-walled steel-to-timber connections using self-tapping screws under shear loading conditions. Their study aimed to evaluate the strength, stiffness, and overall effectiveness of these connections in transferring loads between steel and timber components, further supporting the development of improved design practices for mixed-material constructions. Together, these studies offer a comprehensive view of how different screw connection configurations impact the performance of timber and CFS structures, highlighting the importance of combining high stiffness and ductility in connection designs to enhance the structural reliability of mixed-material systems.

2.7 Timber-timber under cyclic loading

Taylor et al. (2020) investigated the effectiveness of surface spline connectors in Cross-Laminated Timber (CLT) panels when subjected to cyclic shear forces, simulating the effects of seismic events. The study focused on evaluating the performance of these connectors by applying cyclic loads to CLT panels and assessing their strength, stiffness, and failure modes under repeated shear loading. Their findings provided valuable insights into the behaviour of surface spline connections, contributing to the optimization of connection designs to improve the performance and safety of CLT structures in dynamic loading scenarios. Similarly, Chui et al. (2005) explored the performance of timber moment connections under reversed cyclic loading, which is crucial for evaluating the seismic resilience of timber structures. The research aimed to develop and validate a predictive model for the behaviour of timber moment connections subjected to reversed cyclic forces, which mimic the loads experienced during seismic events. The findings from both studies are significant for enhancing the design and assessment of timber structures in seismic regions, offering strategies for improving resilience by accurately modeling and optimizing connection behaviour under dynamic and cyclic loads.

2.8 Connection using different fasteners in Cyclic Loading

Schneider et al. (2015) conducted a comprehensive assessment of the seismic resistance of CLT connections through both experimental and analytical modeling, encompassing 98 tests with various brackets and fasteners. Their study demonstrated a strong correlation between test and model results, particularly in evaluating ductility, elastic shear stiffness, and maximum forces under cyclic loading, while also calibrating an energy-based damage assessment model to link physical damage with energy dissipation. Similarly, Zhou et al. (2014) evaluated the seismic low-cycle fatigue of welded beam-to-column connections in steel moment-resisting frames, accurately predicting the progression of fatigue damage during earthquake conditions and identifying critical connections prone to failure. Closen (2012) examined the behavior of self-tapping screws under different loading conditions, including monotonic loading for static conditions and reverse cyclic loading for dynamic conditions, revealing the need for enhanced design and testing methods for screw assemblies in dynamic environments. Gavric et al. (2014) also investigated the performance of metal connectors such as bolts and screws in CLT structures under cyclic loading, offering valuable insights into their stiffness, strength degradation, and failure modes, thereby contributing to guidelines for improving the durability and safety of timber structures exposed to dynamic forces. Similarly, Mashaly et al. (2011) utilized finite element (FE) analysis to study the behavior of beam-to-column joints in steel frames subjected to cyclic loads, providing critical data for improving the design of steel connections in seismic zones. Oktavianus et al. (2015) introduced a novel connection design incorporating blind bolts, concrete-filled circular hollow steel (CFCHS) columns, and a replaceable energy-dissipating device aimed at enhancing seismic performance and minimizing damage during earthquakes. Their research highlights the potential for developing low-damage, moment-resisting connections that not only improve seismic resilience but also facilitate post-earthquake repair processes, marking a significant contribution to the field of earthquake-resistant design.

2.9 Current Design standards

NZS 3404:2021 for steel structures, incorporates guidelines for cyclic loading specifically relevant to CFS connections to hot rolled steel using self-drilling screws. The code (NZS 3404:2021) outlines the need for

these connections to be designed with sufficient strength and ductility to withstand repeated loading cycles, such as those from seismic activities. It includes provision for fatigue analysis and detailed connection design to maintain structural integrity under cyclic loading conditions, ensuring safety and durability in seismic prone areas. AS/NZS 4600:2018 outlines the requirements for ensuring these connections can withstand cyclic loading, such as seismic forces, by specifying criteria's for strength, stiffness and durability. It emphasises the need for detailed design to account for the effects of repeated loading on screws and connections including factors like fatigue resistance and deformations limits, to ensure the durability and safety of the structure under dynamic conditions. FEMA 461 (FEMA 2007) is used to identify the loading protocol for cyclic loading. According to the FEMA 461 standards (FEMA 2007), it is important to conduct monotonic loading initially to know about the maximum and minimum displacement that could be used for the cyclic loading to determine the displacement of 20 cycles as shown in the Figure (3 and 4)

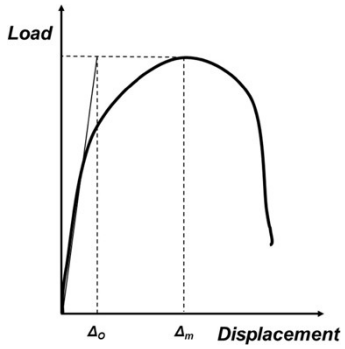

Fig. 3. Schematic representation of estimates from monotonic test results (Danquah et al. 2021)

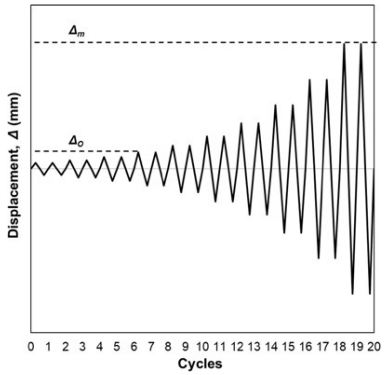

Fig. 4. Schematic cyclic displacement protocol in accordance with FEMA 461 (Danquah et al. 2021)

2.10 Research Gap

- The connection between CFS channel section towards the hot rolled steel is not accurately studied until recent times.
- There are only limited reference papers to identify and certify about the failure modes of these connections.
- Screw connectors in CFS to Steel is relevant for the industry as they help in reducing the time consumption for construction.
- So the performance of screw as connectors it is relevant to conduct cyclic testing for steel to CFS channels using screws and conduct cyclic loading.
- Design guidelines are also limited in this area of research.

2.11 Research objectives

- Behaviour of single and double shear lap connections of screw in 8mm, 12mm, 16mm and 20mm steel material under monotonic and cyclic loading
- Finding the peak load and displacement during monotonic testing and finding the failure modes
- Find the influence of screw parameters in failure
- Finding the influence of steel thickness in failure
- Find the maximum positive and negative loads during cyclic loading
- Find the maximum positive and negative displacement in cyclic loading

3. Material Testing

3.1 Introduction

The material properties of steel, and CFS were determined by conducting a series of material tests. These components were used to fabricate and test steel-steel connections in which the steel-to-steel geometry, screw type, and number of screws were varied. All tests were carried out in the laboratory at the University of Waikato. Detailed information is provided in the sections below.

3.2 Material property of CFS

For steel, three repetitive tensile tests were conducted per ASTM E8-21. The test steel coupons were extracted from the web thickness of the C Channel section of 1.80 mm thickness as shown in Figure 5 the coupons of size 2.0 mm width, 2.0 mm thick, and 19.6 mm gauge length were prepared using Wire EDM. Tensile tests were carried out on a 5 kN Instron machine under displacement/force control at a displacement/loading rate of 1mm/min. Figure 6. and Table 1. present the stress-strain response and the main mechanical parameters for each tested coupon, such as the yield strength (σy), the ultimate tensile strength (σu), and the elongation at fracture (εf).

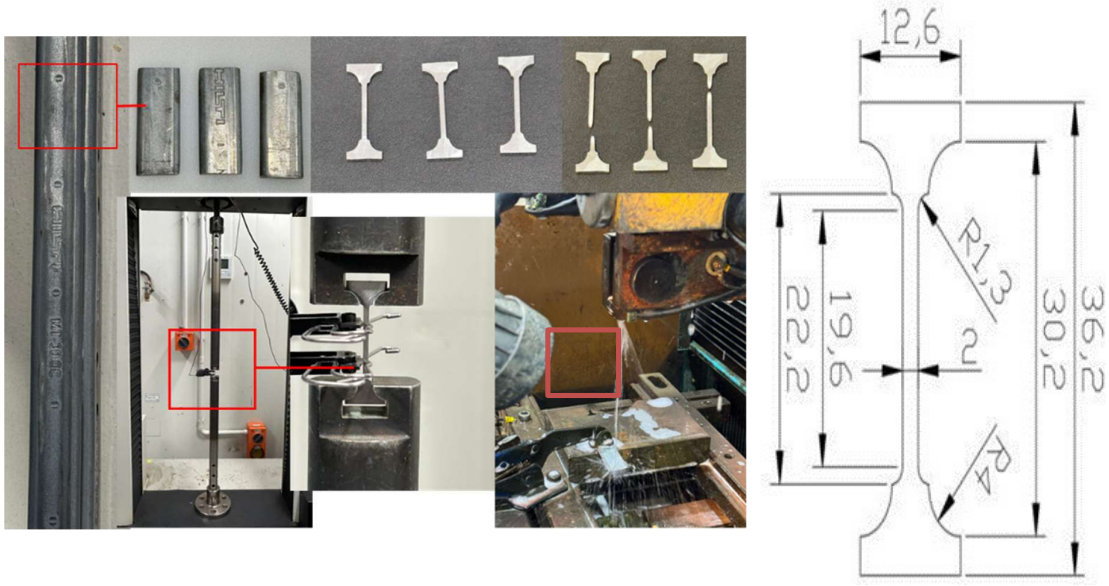

Figure 5 CFS coupon sample preparation

Table 1 Material property of CFS

Steel Coupon	Yield Strength σy (MPa)	Tensile strength σu (MPa)	Elongation at fracture εf (%)	Average yield strength σy (MPa)	Average tensile strength σu (MPa)	Average elongation at fracture εf (%)
SC-01	367.52	435.03	92.92	371.27	432.69	91.54
SC-02	368.89	428.99	86.53			
SC-03	377.39	434.04	95.17			

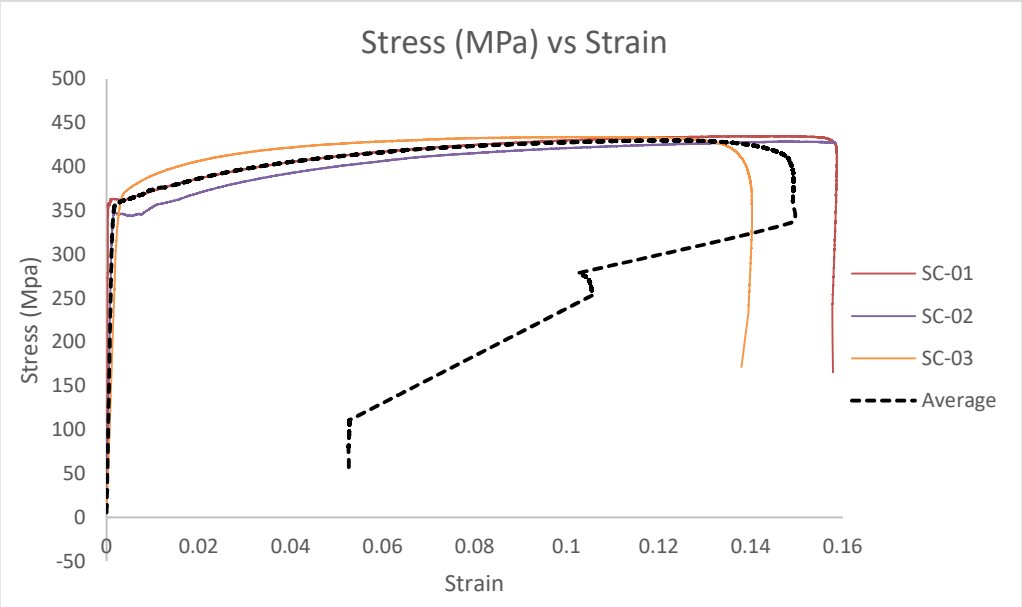

Figure 6 Stress-strain graphs for CFS used in the experiments.

3.3 Material property of structural steel

For steel, three repetitive tensile tests were conducted per ASTM E8-21. The test steel coupons were extracted from a steel plate of 12.0 mm thickness as shown in Figure 7 the coupons of size 2.0 mm width, 2.0 mm thick, and 19.6 mm gauge length were prepared using Wire EDM. Tensile tests were carried out on 5 kN Instron machine under displacement/force control at a displacement/loading rate of 1mm/min. Figure 8 and Table 2 present the stress-strain response and the main mechanical parameters for each tested coupon, such as the yield strength(σy), the ultimate tensile strength (σu), and the elongation at fracture (εf).

Figure 7 Steel coupon sample preparation.

Table 2 Material property of steel

Steel coupon	Yield strength σy (MPa)	Tensile strength σu (MPa)	Elongation at fracture εf (%)	Average yield strength σy (MPa)	Average tensile strength σu (MPa)	Average elongation at fracture εf (%)
SC-01	422.88	565.53	12.11			
SC-02	445.60	569.02	16.7	433.66	568.23	14.77
SC-03	432.5	570.13	15.5			

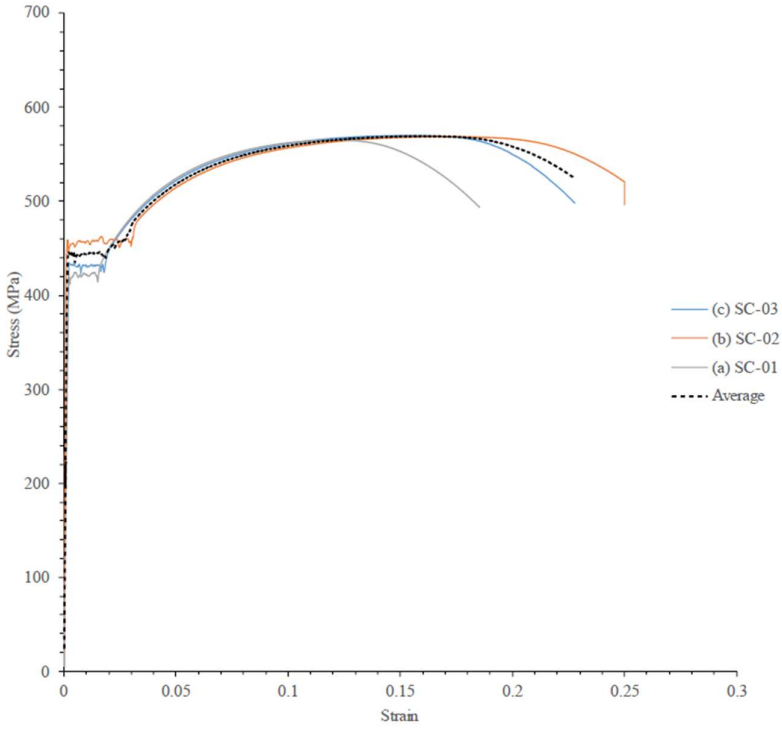

Figure 8 Stress-strain graphs for steel plates used in the experiments.

4. Specimen Description and Testing Arrangements

4.1. Introduction

This chapter's goal is to go over the specifics of the specimens utilised in the testing, such as self-drilling screws, structural steel, and CFS. There is also discussion of the testing setups, equipment, and rigs.

4.2. Specimen Construction

The steel plates have four different thicknesses of 8 mm, 12 mm, 16 mm, and 20 mm, and a length of 300 mm and a width of 100 mm as shown in Figure (9). CFS thickness of 1.8mm, with a depth of 41 mm, width of 23 mm, mouth width of 22 mm, rebate height of 7.5 mm, centre to centre distance from hole is 100 mm, diameter of hole is 12 mm as shown in Figure (10) and length were 300mm for single screw connection and 360mm for double screw connection. The screws are made of steel having a zinc plated surface having a nominal diameter of 6.3 mm. The physical features of the screw are mentioned in Table 3

Figure 9 Hot rolled steel

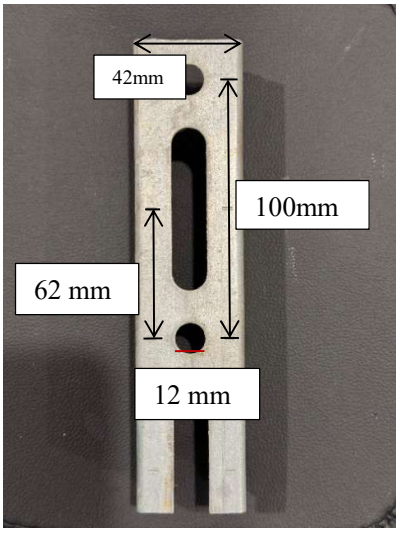

Figure 10 CFS Specimen

Table 3 Physical features of screws

Surface	Head Type	Thread type	Nominal Diameter (mm)	Length (mm)	Head Diameter (mm)	Drill tip Length (mm)	Screw-thread length with drill tip (mm)
Zinc plated	Hexagonal Head	Self-tapping screw thread	6.3	38	13.3	8.5	33.5

The cyclic test was conducted on specimens incorporating structural steel, CFS materials and screws. In all configurations, screws were employed to establish a connection between the steel and CFS. The 6.3 mm diameter screw head Figure (11) were aligned with the top of CFS element and the threaded part passed through the steel element as shown in Figure (12). The screw was drilled into the composite structure keeping the screw head in contact with the CFS. The parameters evaluated in the test were: (i) steel plate thickness, and (ii) number of screws.

Figure 11 Hexagonal Screw head.

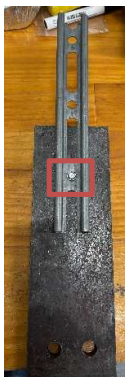

Figure 12 Steel-CFS Connection.

CFS thickness of 1.8 mm, with the width of 42 mm and length were 300 mm and 360 mm respectively. For the single screw connection, the screws are positioned 70 mm from the end of the CFS plate. For the two-screw connection, the two screws were positioned 30 mm from the end of the CFS and 100 mm from the centre to the centre as shown in Figure (13). For M16 bolts, which were used to connect to the rig, two parallel holes were made in the steel plate at a distance of 30 mm from one end as shown in Figure (14).

Figure 13 Double Screw connection

Figure 14 Parallel holes in steel plate for M16 bolts.

The specimens are labelled according to steel thickness (8, 12, 16, 20 mm), CFS thickness (1.8 mm), and number of screws. For example, S08-CFS1.8-N1 indicates: S08 is for the steel with a thickness of 8 mm, CFS1.8 means CFS with 1.8 mm thickness, N1 is one screw of diameter 6.3 mm.

4.3. Testing Arrangement and Instrumentation

Two custom test rigs were constructed to replace the grips of the machine and to enable the test specimens to be bolted to the 100 kN Instron as shown in Figure (15). The steel-CFS specimen were fastened to the rigs using M16 and M12 bolts respectively, in which the steel plate is connected to the bottom rig, while the CFS is connected to the test rig. A test specimen of the test rigs for the cyclic test is shown in Figure (16).

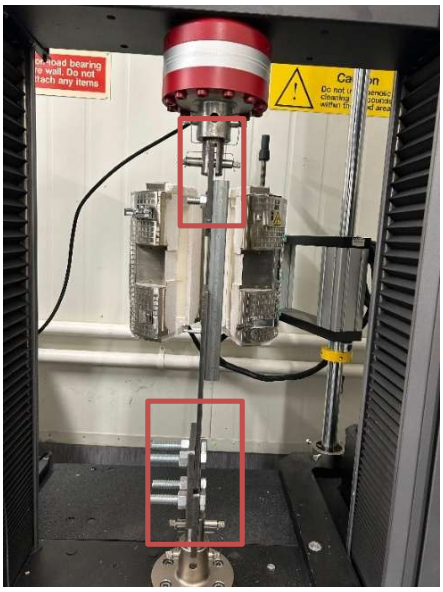

Figure 15 Specimen arrangements

Figure 16 Test rigs

5. Specimen Loading

5.1. Introduction

The purpose of this chapter is to present the experimental investigation program for the cyclic strength of self-drilling wing screws in structural steel-to-CFS. Cyclic tests were performed to investigate the design values of load deformation. The tests included a comprehensive set of combinations of different steel thicknesses and CFS in the most suitable configuration. All joint specimens were first tested using a monotonic displacement protocol, with load-displacement results used to determine the appropriate cyclic loading protocol in accordance with Federal Emergency Management Agency (FEMA) 461 (FEMA 2007).

5.2. Loading Protocol

Monotonic tests were loaded at a constant displacement rate of 0.025 mm/sec. The cyclic loading protocol is adopted from the FEMA 461 quasi-static cyclic deformation-controlled testing protocol (FEMA 2007) (Tao et al. 2016) as Figure (17), which was developed to obtain fragility data and hysteretic response characteristics of building components for which damage is best predicted by imposed deformations. The protocol defines two cycles at equal displacement amplitude per step.

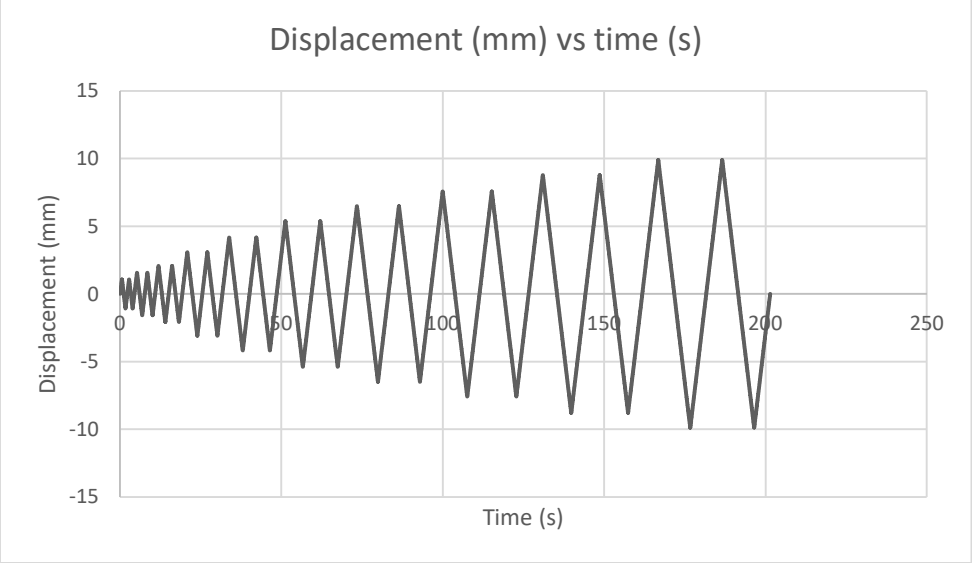

Figure 17 Displacement vs. Time Graph.

The starting displacement amplitude is determined based on an estimate of the deformation corresponding to damage initiation Δ_o, FEMA 461 requires a minimum of six displacement cycles prior to reaching Δ_o. The targeted deformation corresponding to maximum load Δ_m, is also required to be defined for which a minimum of ten displacement cycles are required prior to reaching. The two deformation values Δ_o and Δ_m are determined from a performed monotonic test: Δ_o is determined from assuming that the test specimen remains elastic based on the secant stiffness up to the peak load, and Δ_m is determined as displacement corresponding to the peak load, as shown in Figure (18)

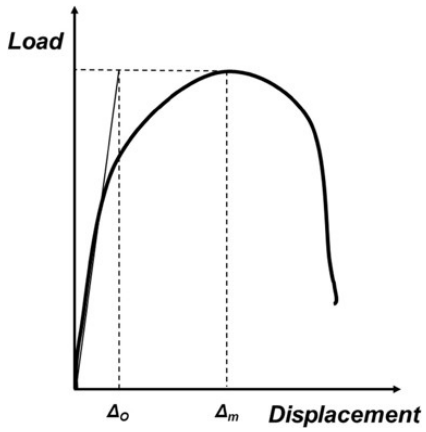

Fig. 18. Schematic representation of estimates from monotonic test results

Joint specimens using screws were then tested under the quasi-static cyclic displacement protocol. Additionally, screw-fastened joints were also tested following the same cyclic displacement protocol of the quasi-static tests, with a load rates 2 mm/s (Danquah et al. 2021).

6. Fastener load-deformation monotonic and cyclic response

6.1. Fastener load-deformation backbone nomenclature

Backbone curves are used to characterize monotonic and cyclic fastener load deformation response for developing hysteretic models with strength and stiffness degradation. The backbone configuration (Figure 18) is inspired by the Ibarra-Medina-Krawinkler Model (2005), and each curve consists of five regions: elastic, hardening, peak, post peak, and residual. Each region is defined by its associated load

and displacement points ((ePd_1,ePf_1), (ePd_2,ePf_2), (ePd_3,ePf_3), and (ePd_4,0)) for positive region and ((eNd_1,eNf_1), (eNd_2,eNf_2), (eNd_3,eNf_3) and (eNd_4,0)) for the negative region and related stiffness (slope) Ke, Ks, Kc, and Kr as shown in Figure (19)

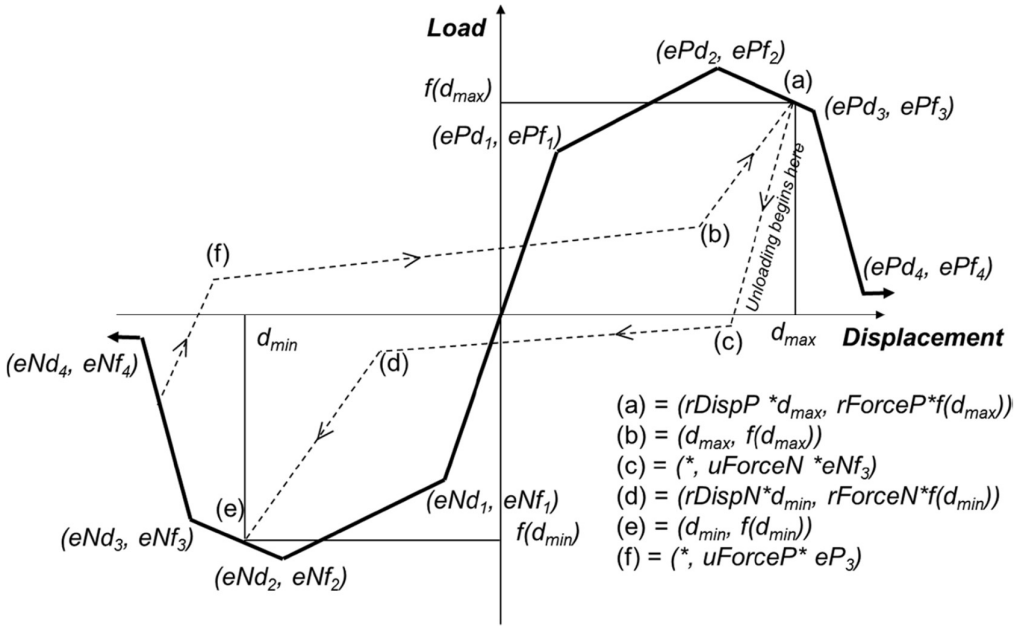

Fig. 19. Backbone curve nomenclature (Danquah et al. 2021)

6.2. Fastener load-deformation backbone construction procedure

Monotonic backbone construction was performed by visually selecting (ePd_2,ePf_2) as the first peak load after hardening, them visually selecting (ePd_1,ePf_1) to match the elastic and hardening slopes, Ke and Ks, respectively. The point (ePd_3,ePf_3) is obtained so that the post peak backbone segment from (ePd_2,ePf_2) to (ePd_3,ePf_3) is a linear fit (ie; the average) of the tested response and then ePd_3, is calculated by equating the energy dissipation of the tested load-displacement curve and backbone response. The backbone of the positive and negative cyclic response (Figure 20) was obtained by first identifying the response outline with the Matlab backbone command (Matlab 2015) with the shrink factor equal to 1 and then following the same monotonic backbone construction procedure.

Backbones are constructed for each steel-CFS combinations and for both monotonic and cyclic loading. Tables of all backbone parameters and the statistics based on the average of the three trials are included in Table 4, where M represents the monotonic loading

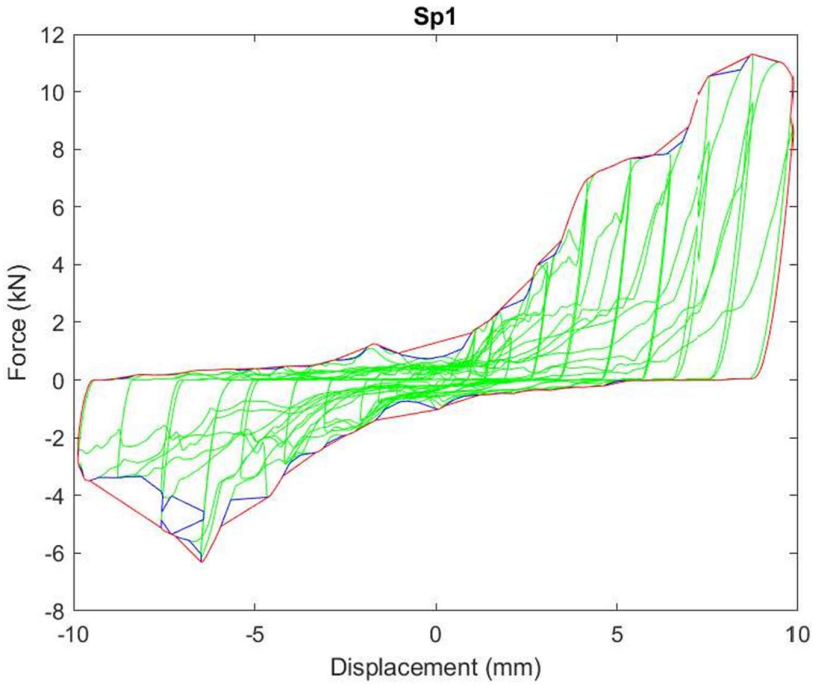

Fig. 20. Cyclic backbone response

Table 4 Backbone parameters for monotonic testing

TEST	LOADING		ePd_1	ePd_2	ePf_1	ePf_2	Ke	Ks
ST08-CFS1.8-N1	M	Mean	2.96	9.80	3.47	11.37	1.17	1.17
		Cov	12.06	11.04	27.34	4.56	25.83	11.36
ST12-CFS1.8-N1	M	Mean	3.93	10.43	3.52	11.33	0.90	1.23
		Cov	2.45	13.14	3.10	7.54	3.23	20.07
ST16-CFS1.8-N1	M	Mean	3.17	10.18	2.76	11.08	0.87	1.19
		Cov	8.30	13.56	13.56	2.18	13.56	7.83
ST20-CFS1.8-N1	M	Mean	3.62	10.14	4.54	11.51	1.26	1.07
		Cov	5.97	6.00	11.05	1.49	16.14	8.11
ST08-CFS1.8-N2	M	Mean	6.63	13.33	7.90	17.35	1.19	1.42
		Cov	3.36	7.39	14.23	1.02	12.64	16.31
ST12-CFS1.8-N2	M	Mean	4.66	12.74	8.92	16.93	1.92	0.99
		Cov	9.12	5.41	6.92	1.63	3.03	5.75
ST16-CFS1.8-N2	M	Mean	4.03	13.18	6.84	17.02	1.75	1.11
		Cov	19.15	10.14	6.39	1.89	25.17	1.69
ST20-CFS1.8-N2	M	Mean	4.65	12.10	9.04	16.58	1.96	1.01
		Cov	10.13	3.33	1.35	0.74	8.84	1.90

6.3. Fastener load-deformation response for steel-CFS specimen

An example set of steel-to-CFS backbone is shown in Figure (21). This combination failed through fastener screw shear, which is evident in the large drop in load with a small displacement change. In the specimen ST08-CFS1.8-N1 as the displacement was 8.77mm the maximum load was obtained as 11.92

kN and as the displacement changes to 9.00mm there was a drop in load to a value of 11.62kN. Depending on the combination, the specimen failed in fastener screw shear, bearing or fastener screw pullout after tilting.

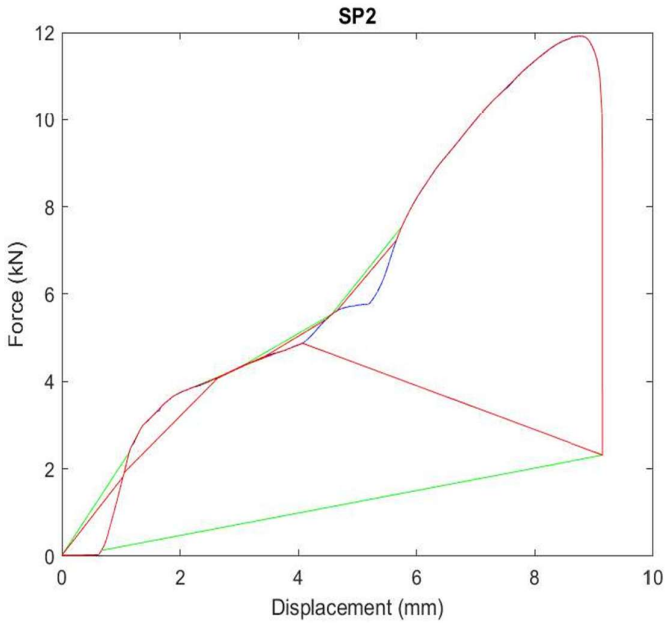

Fig. 21. Monotonic Backbone response

7. Monotonic Test Results

This section presents the experimental investigation program for the shear strength of self-drilling screw in steel to CFS. Monotonic tests were performed to investigate the design values of shear connection to find the minimum and maximum displacement for cyclic testing. The test includes a comprehensive set of combination of different steel samples and variation of number of screws.

To get the results regarding the deformation corresponding to damage initiation and the deformation corresponding to maximum load, monotonic testing was carried out for both single and double screw connections. The Table 5 discusses all of the findings about the two specimen setups. The values for each cyclic count could be examined once the table was evaluated. The screw had a shear failure, as depicted in the Figure (22), during the single screw connection testing procedure. As seen in the Figure (23), CFS specimens tend to distort. At the point of final failure, some of the specimens have bearing and tear out failure.

Table 5 Monotonic test results

TEST		Ultimate Load (kN)	Displacement (mm)	Failure Mode
ST08-CFS1.8-N1	Mean	11.37	9.79	S.S
ST12-CFS1.8-N1	Mean	11.79	10.43	S.S
ST16-CFS1.8-N1	Mean	11.09	10.18	S.S
ST20-CFS1.8-N1	Mean	11.52	10.14	S.S
ST08-CFS1.8-N2	Mean	17.36	13.33	B/T
ST12-CFS1.8-N2	Mean	17.00	12.74	B/T
ST16-CFS1.8-N2	Mean	17.04	13.18	B/T
ST20-CFS1.8-N2	Mean	16.59	12.10	B/T

Fig. 22. Screw Failure

Fig. 23. CFS specimen deformation

For single screw connection the average peak load ranges from a lowest load of 11.09 kN for ST16-CFS1.8-N1 to a highest load of 11.79 kN for ST12-CFS1.8-N1 The average peak displacement ranges from a lowest value of 9.79 mm for ST08-CFS1.8-N1 to a highest value of 10.43 mm for ST12-CFS1.8-

N1. For double screw connection the average load ranges from a lowest load of 16.59 kN for ST20-CFS1.8-N2 to a highest load of 17.36 kN for ST08-CFS1.8-N2. The average peak displacement ranges from a lowest value of 12.10 mm for ST20-CFS1.8-N2 to a highest value of 13.33 mm for ST08-CFS1.8-N2.

7.1. Influence of screw parameters

All the test results of the experiment of shear connection were recorded and are presented in Table (5) including the type of failure mode that occurred for each specimen together and the corresponding ultimate capacity as shown in Figure (24). The failure is responded as S.S which is screw shear failure and B/T for bearing and tear out failure. For all the tests, CFS surface failure was noticeable. Even though the test specimens exhibited different failure modes, all the specimen's ultimate failure in shear. As the number of screws increased from single to double screw there was an average increase of 48.55% in capacity.

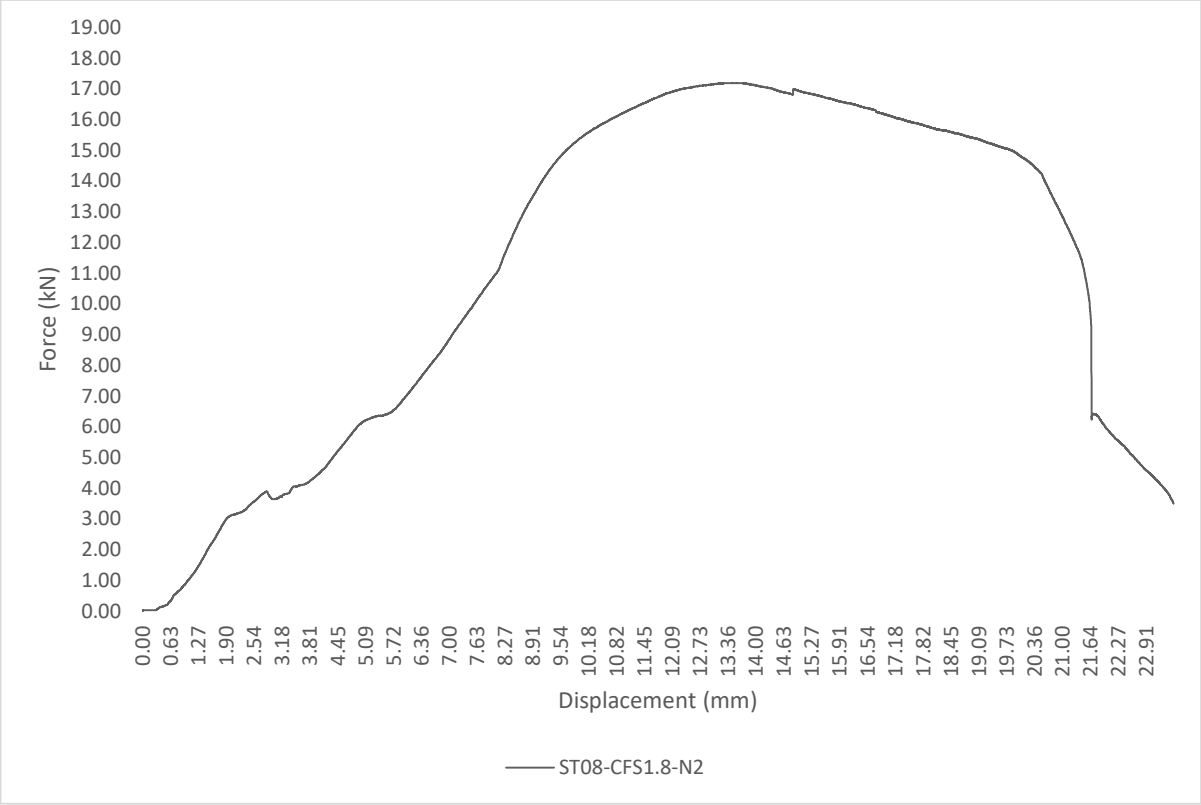

Fig. 24. Monotonic load vs displacement

7.2. Effect of steel thickness

An effect in either peak load or stiffness has been found in steel-to-CFS connections when thicker steel is used. According to the graph in Figure (25-28), as the steel thickness was increased from 8mm to 12 mm the capacity was increased to 3.69% and as the steel thickness increased to 16 mm the capacity was decreased to 2.46% and as the thickness was increased to 20mm the capacity increased to 1.32%, there is an average increase of 1.31% in capacity as the steel thickness increase from 8 mm to 20 mm for a single screw connection. For double screw connection as the steel thickness was increased as 8 mm,12 mm, 16 mm, and 20 mm, the average capacity was increased to 2.07%, 1.84%, 4.43% accordingly.

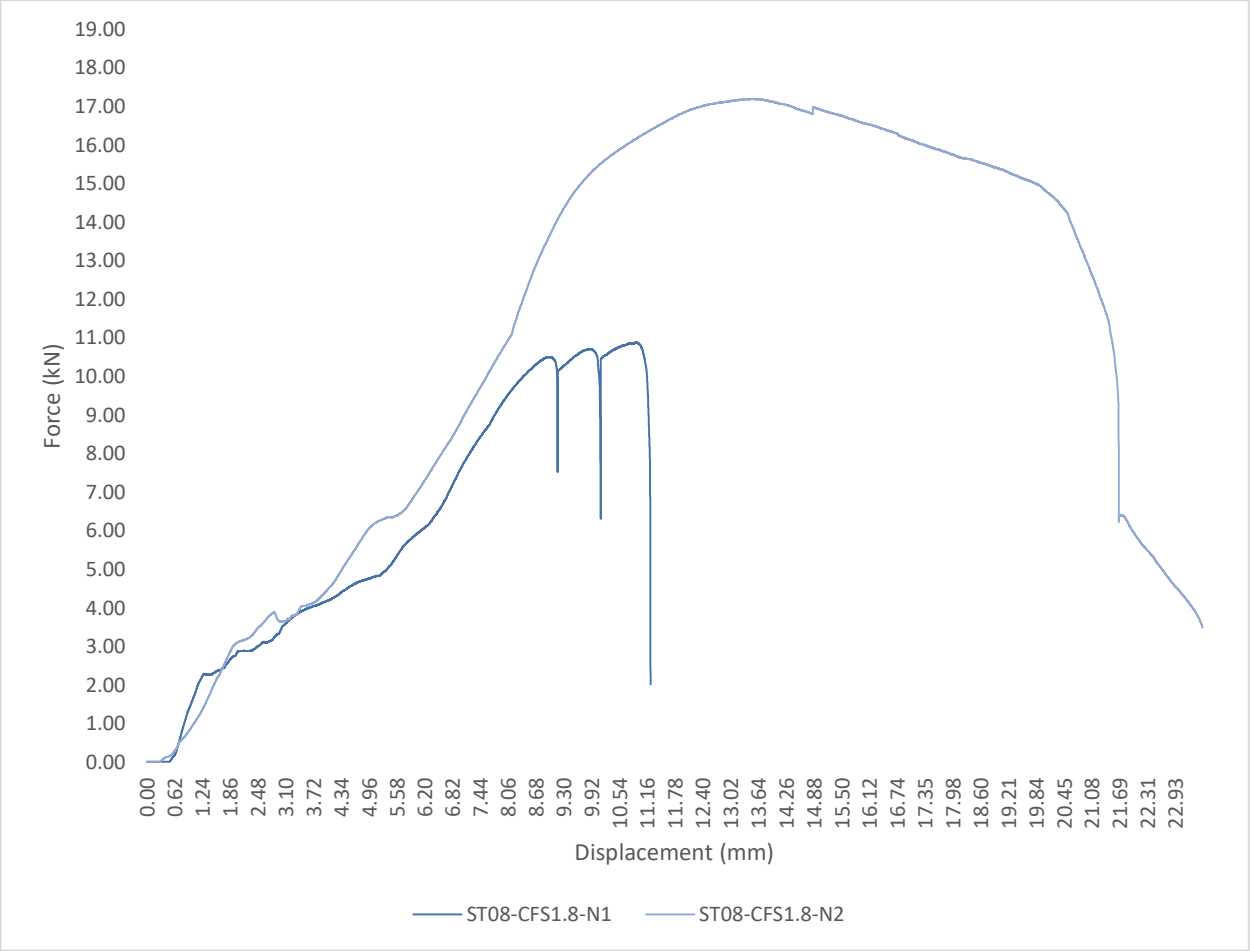

Fig. 25. The load-displacement curve for 8 mm steel plate

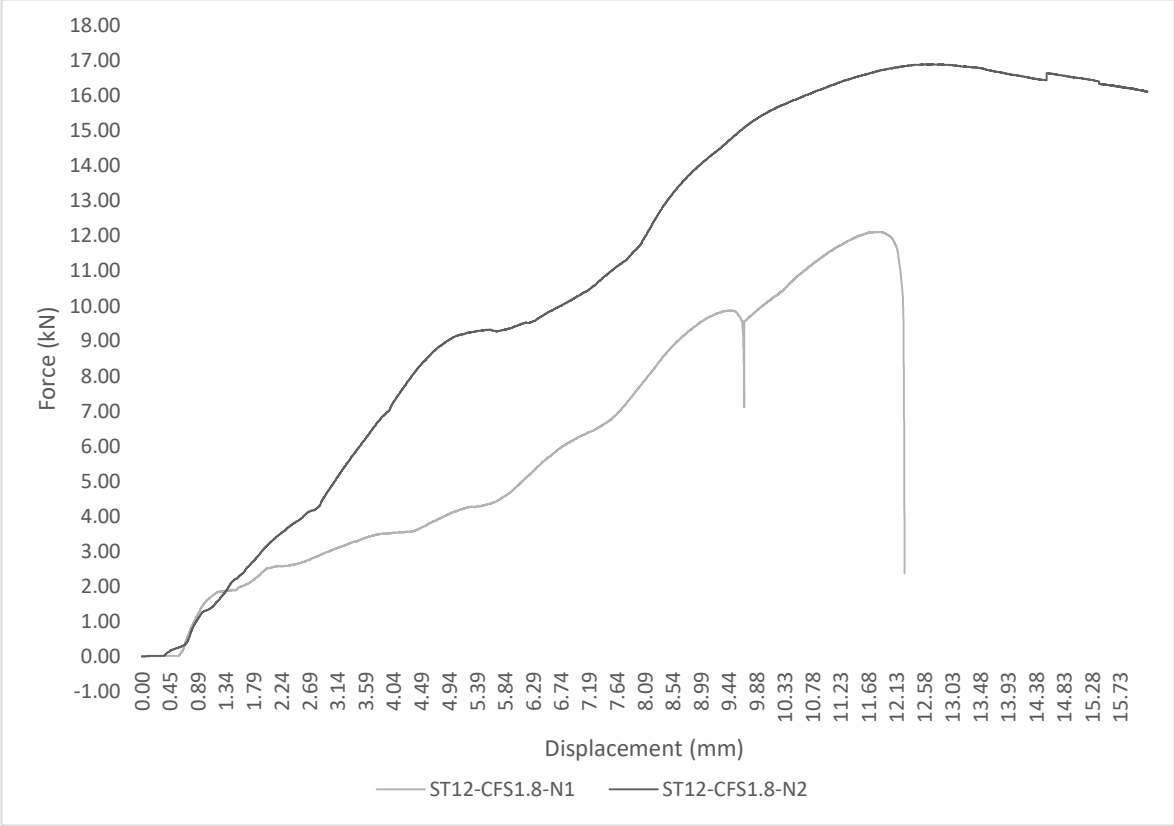

Fig. 26. The load-displacement curve for 12 mm steel plate

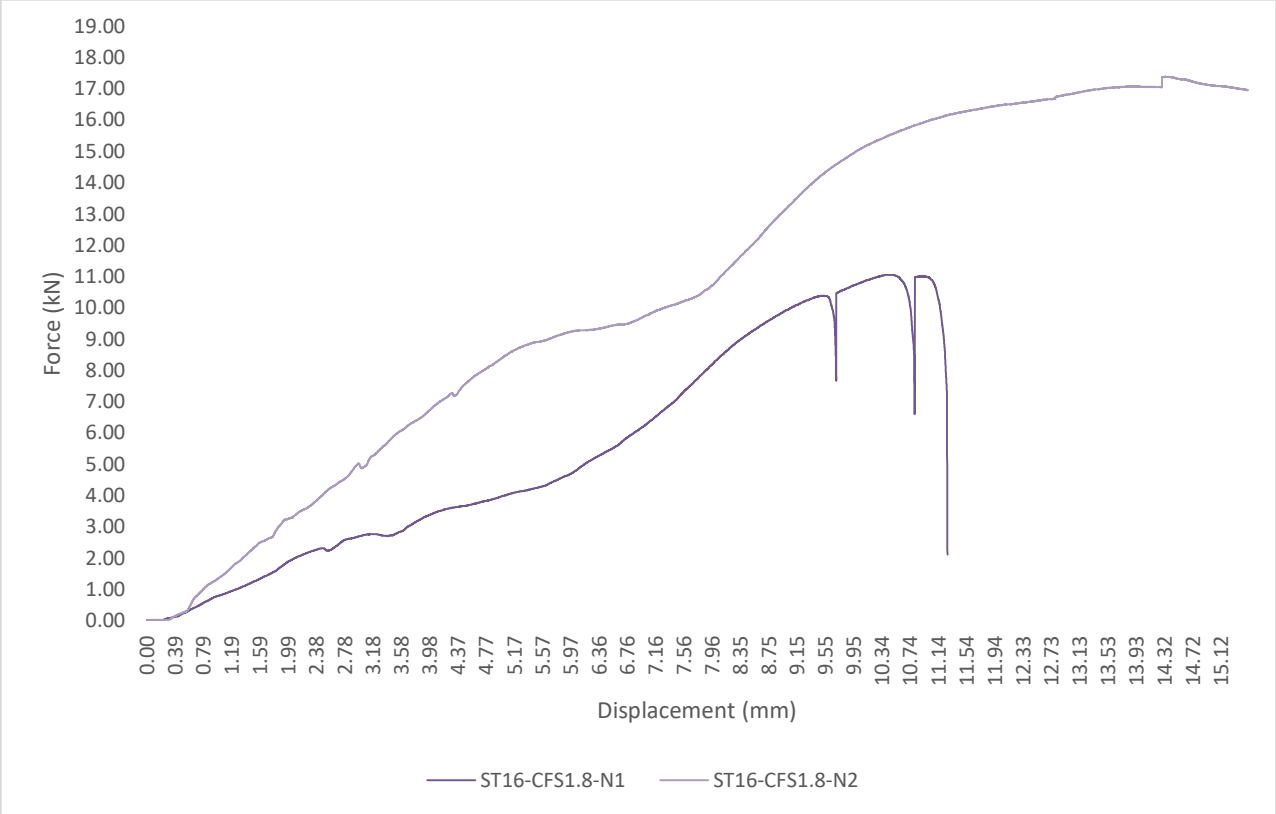

Fig. 27. The load-displacement curve for 16 mm steel plate

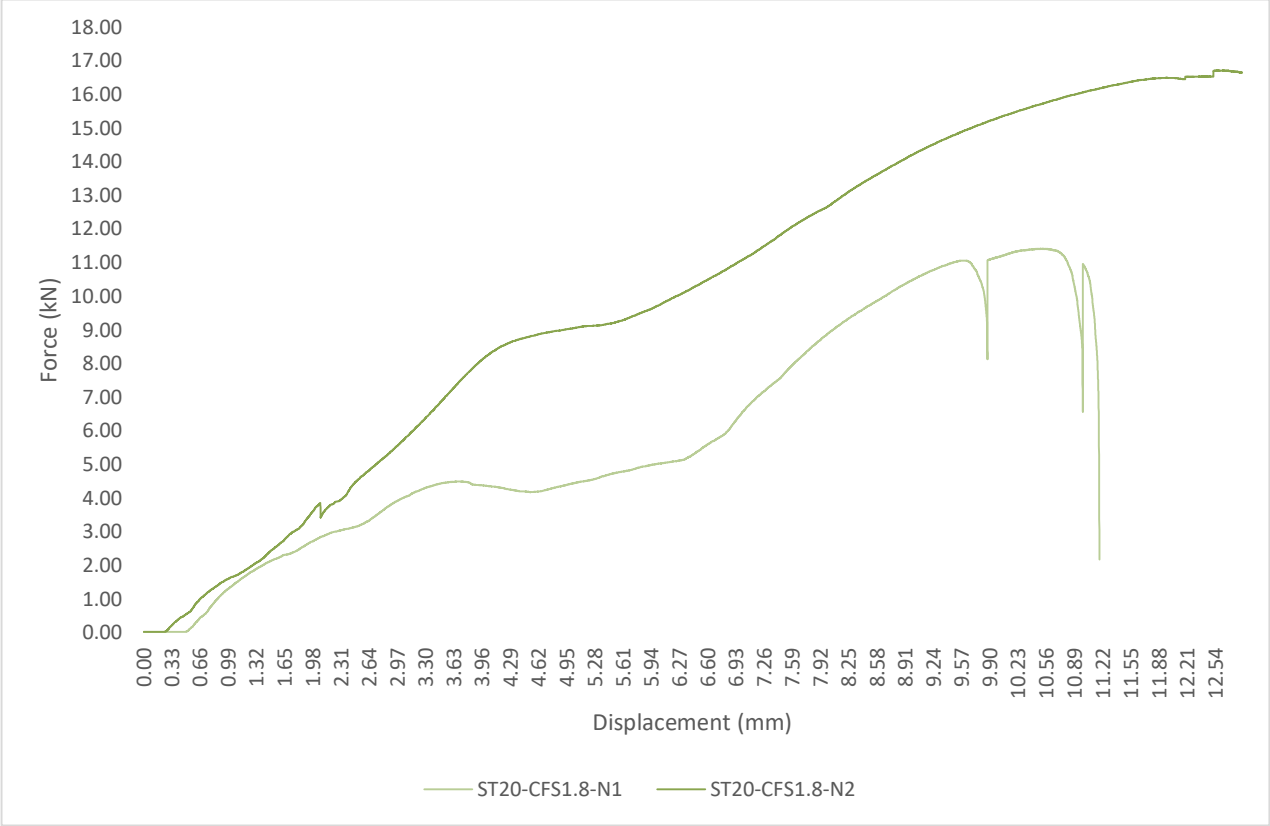

Fig. 28. The load-displacement curve for 20 mm steel plate

7.3. Load displacement relationship

For the loading stages of all the test specimens, the initial slip was observed because of the rigs bolt, resulting in a small flat line before elastic deformation. The specimen showed elastic deformation up to the maximum strength after which non-linear behaviour was observed. At an average displacement of 10.135 mm, most of the specimens failed in a single screw connection, and at an average displacement of 12.84 mm most of the specimen s failed in a double screw connection. Due to the formation of the plastic hinge of the screw, several peaks were observed in the load-displacement curve.

8. Cyclic Test Results

The experimental study program for the cyclic testing of self-drilling screws in steel-to-CFS is presented in this part. To discover relevant values about cyclic testing, cyclic tests were performed on a total of 24 specimens. For each set of specimen arrangements, three sets of tests were conducted again. For cyclic testing, a total of 20 cycles were performed. The results were used to calculate values such as post peak, elastic and hardening slope, and peak load.

The results of the monotonic testing were used to determine the displacement values. For ST16-CFS1.8-N1, the maximum monotonic testing was 14 mm. Table 12 displays the results for quantities such as ePd1, which represents displacement at the positive elastic hardening point, and ePf1, which represents force at the same location. ePd2 for the displacement at peak load and ePf2 for the positive force. The post-peak positive displacement and force are represented by ePd3 and ePf3, while the residual displacement and force are represented by ePd4 and ePf4. Together with the findings in Tables 6 and 7, the negative displacement and forces are also covered. The negative displacement and force at the elastic hardening point under compression are denoted by eNd1 and eNf1. Negative displacement and force at peak negative load are represented by eNd2 and eNf2, respectively, whereas negative displacement and force at post-peak loading are represented by eNd3 and eNf3, as shown in Tables 8 and 9. The residual values at compression are eNd4 and eNf4. For every test specimen, ePf4 and eNf4 are shown to be zero in these data.

Table 6 Positive displacement backbone parameters

Test		ePd1 (mm)	ePd2 (mm)	ePd3 (mm)	ePd4 (mm)
ST08-CFS1.8-N1	Mean	4.009	9.257	9.792	9.125
	CoV	0.059	0.060	0.004	0.069
ST12-CFS1.8-N1	Mean	5.415	10.344	10.453	9.546
	CoV	0.305	0.012	0.006	0.042
ST16-CFS1.8-N1	Mean	3.744	9.863	10.129	9.359
	CoV	0.223	0.070	0.019	0.087
ST20-CFS1.8-N1	Mean	2.987	9.798	10.232	9.371
	CoV	0.154	0.059	0.004	0.063
ST08-CFS1.8-N2	Mean	3.754	12.625	13.377	12.037
	CoV	0.077	0.049	0.000	0.003
ST12-CFS1.8-N2	Mean	4.492	12.757	12.826	11.397
	CoV	0.067	0.005	0.000	0.010
ST16-CFS1.8-N2	Mean	4.369	13.244	13.278	11.808
	CoV	0.119	0.000	0.000	0.005
ST20-CFS1.8-N2	Mean	4.479	12.145	12.173	10.574

	CoV	0.068	0.000	0.000	0.007

Table 7 Positive force backbone parameters

Test		ePf1 (mm)	ePf2 (mm)	ePf3 (mm)	ePf4 (mm)
ST08-CFS1.8-N1	Mean	5.503	11.648	9.360	0.000
	CoV	0.229	0.025	0.021	
ST12-CFS1.8-N1	Mean	3.736	10.469	8.997	0.000
	CoV	0.114	0.052	0.052	
ST16-CFS1.8-N1	Mean	4.737	9.536	8.635	0.000
	CoV	0.108	0.133	0.150	
ST20-CFS1.8-N1	Mean	4.456	10.724	8.654	0.000
	CoV	0.129	0.026	0.103	
ST08-CFS1.8-N2	Mean	6.815	16.286	14.165	0.000
	CoV	0.201	0.005	0.005	
ST12-CFS1.8-N2	Mean	7.270	16.415	14.629	0.000
	CoV	0.078	0.008	0.013	
ST16-CFS1.8-N2	Mean	9.897	17.086	15.137	0.000
	CoV	0.032	0.013	0.035	
ST20-CFS1.8-N2	Mean	8.990	16.643	14.970	0.000
	CoV	0.167	0.036	0.036	

Table 8 Negative displacement backbone parameters

Test		eNd1 (mm)	eNd2 (mm)	eNd3 (mm)	eNd4 (mm)
ST08-CFS1.8-N1	Mean	-2.793	-5.815	-6.822	-8.271
	CoV	-0.580	-0.117	-0.092	-0.133
ST12-CFS1.8-N1	Mean	-4.683	-9.626	-9.697	-9.967
	CoV	-0.144	-0.045	-0.070	-0.043
ST16-CFS1.8-N1	Mean	-2.683	-6.571	-4.985	-8.581
	CoV	-0.344	-0.456	-1.020	-0.110
ST20-CFS1.8-N1	Mean	-3.599	-7.688	-9.869	-8.944
	CoV	-0.210	-0.296	-0.064	-0.072
ST08-CFS1.8-N2	Mean	-4.496	-13.345	-13.308	-11.912
	CoV	-0.211	0.000	-0.005	-0.002

ST12-CFS1.8-N2	Mean	-4.316	-12.795	-12.807	-11.320
	CoV	-0.223	0.000	-0.002	-0.004
ST16-CFS1.8-N2	Mean	-5.486	-13.245	-13.277	-11.721
	CoV	-0.026	0.000	0.000	-0.009
ST20-CFS1.8-N2	Mean	-5.327	-12.156	-12.083	-10.730
	CoV	-0.146	-0.001	-0.001	-0.020

Table 9 Negative force backbone parameters

Test		eNf1 (kN)	eNf2 (kN)	eNf3 (kN)	eNf4 (kN)
ST08-CFS1.8-N1	Mean	-2.479	-4.378	-3.450	0.000
	CoV	-0.317	-0.384	-0.452	
ST12-CFS1.8-N1	Mean	-3.239	-7.127	-5.129	0.000
	CoV	-0.151	-0.166	-0.155	
ST16-CFS1.8-N1	Mean	-2.319	-3.389	-2.738	0.000
	CoV	-0.168	-0.420	-0.252	
ST20-CFS1.8-N1	Mean	-3.586	-5.038	-3.637	0.000
	CoV	-0.238	-0.289	-0.300	
ST08-CFS1.8-N2	Mean	-8.304	-18.615	-15.405	0.000
	CoV	-0.203	-0.009	-0.100	
ST12-CFS1.8-N2	Mean	-8.470	-18.697	-16.674	0.000
	CoV	-0.027	-0.035	-0.090	
ST16-CFS1.8-N2	Mean	-9.440	-18.620	-16.810	0.000
	CoV	-0.051	-0.057	-0.045	
ST20-CFS1.8-N2	Mean	-7.735	-16.985	-13.637	0.000
	CoV	-0.143	-0.110	-0.112	

Additionally, Table (10) discusses slope values. Ke represents the slope up to the elastic hardening point, Ks represents the slope from the elastic hardening point to the peak load, Kc represents the slope from the peak load to the post-peak load, and Kr represents the slope up to the residual point.

Table 10 Slope

Test		Ke (kN/mm)	Ks (kN/mm)	Kc (kN/mm)	Kr (kN/mm)
ST08-CFS1.8-N1	Mean	1.367	1.160	16.531	-25.242
	CoV	0.192	0.164	2.047	-2.339
ST12-CFS1.8-N1	Mean	0.727	1.439	-15.271	13.012
	CoV	0.295	0.240	-0.340	0.686
ST16-CFS1.8-N1	Mean	1.319	0.785	-123.392	-2.910
	CoV	0.282	0.311	-2.014	-5.848
ST20-CFS1.8-N1	Mean	1.496	0.921	-17.983	20.916
	CoV	0.029	0.114	-1.089	1.120
ST08-CFS1.8-N2	Mean	1.836	1.068	-22.947	10.583
	CoV	0.266	0.141	-1.587	0.026
ST12-CFS1.8-N2	Mean	1.622	1.108	-43.593	10.282
	CoV	0.093	0.066	-0.660	0.085
ST16-CFS1.8-N2	Mean	2.290	0.813	-57.901	10.300
	CoV	0.138	0.091	-0.148	0.022
ST20-CFS1.8-N2	Mean	2.027	1.002	-59.937	9.364
	CoV	0.230	0.152	-0.242	0.032

As seen in the Figure (29), it was found that the majority of the specimens suffered from bearing and tear out failure during cyclic testing. Table (11) lists the modes of failure. According to Danquah et al. (2021), the primary failures noted are S.S., which stands for screw shear failure, and B/T, which indicates bearing and tear out failure.

Fig. 29. Cyclic failure

Table 11 Failure Mode

TEST	Failure Mode
ST08-CFS1.8-N1	B/T
ST12-CFS1.8-N1	B/T
ST16-CFS1.8-N1	B/T
ST20-CFS1.8-N1	B/T
ST08-CFS1.8-N2	B/T
ST12-CFS1.8-N2	B/T
ST16-CFS1.8-N2	B/T
ST20-CFS1.8-N2	B/T

For single screw connection the average positive peak load ranges from a lowest load of 9.54 kN for ST16-CFS1.8-N1 to a highest load of 11.65 kN for ST08-CFS1.8-N1 and the average negative peak load ranges from a lowest load of -3.39 kN for ST16-CFS1.8-N1 to a highest load of -7.13 kN for ST12-CFS1.8-N1. For double screw connection the average positive peak load ranges from a lowest load of 16.29 kN for ST08-CFS1.8-N2 to a highest load of 17.09 kN for ST16-CFS1.8-N2 and the average negative peak load ranges from a lowest load of -16.99 kN for ST20-CFS1.8-N2 to a highest load of -18.70 kN for ST12-CFS1.8-N2

8.1. Influence of screw parameters

All of the test findings from the cyclic testing experiment were documented and are shown in Table 6-9. Table 11 includes the kinds of failure modes that were noted for every specimen. CFS surface failure was evident in every test. All of the test specimens eventually failed in tear out, despite the fact that they showed various failures.

It was found that the specimens tended to fail more slowly as the withstanding capacity increased with the number of screws in the connection. There is an average increase of 56.77% in capacity as the number if screws were increased from single screw to double screw connection. The peak positive and negative loads for each of the test results are shown in Table 12.

Table 12 Cyclic Response

TEST		Positive Displacement (mm)	Peak Positive Load (kN)	Negative displacement (mm)	Peak Negative Load (kN)
ST08-CFS1.8-N1	Mean	9.26	11.65	-5.82	-4.38
	Cov	5.99	2.47	-0.12	-0.38
ST12-CFS1.8-N1	Mean	10.34	10.47	-9.63	-7.13
	Cov	1.22	5.20	-0.05	-0.17
ST16-CFS1.8-N1	Mean	9.86	9.54	-6.57	-3.39
	Cov	7.02	13.32	-0.46	-0.42
ST20-CFS1.8-N1	Mean	9.80	10.72	-7.69	-5.04
	Cov	5.90	2.56	-0.30	-0.29
ST08-CFS1.8-N2	Mean	12.62	16.29	-13.35	-18.62
	Cov	4.94	0.50	0.00	-0.01
ST12-CFS1.8-N2	Mean	12.76	16.42	-12.80	-18.70
	Cov	0.51	0.76	0.00	-0.04
ST16-CFS1.8-N2	Mean	13.24	17.09	-13.25	-18.62
	Cov	0.00	1.31	0.00	-0.06
ST20-CFS1.8-N2	Mean	12.14	16.64	-12.16	-16.99
	Cov	0.00	3.57	0.00	-0.11

8.2. Effect of steel thickness

The use of thicker steel was found to have an impact on both positive and negative peak loads in steel-CFS connections. The graph in Figure (30-33) shows that, as the steel thickness was increased as 8 mm, 12 mm, 16 mm, and 20 mm, the average capacity was reduced to 10.13%, 18.11%, 7.98% accordingly for a single screw connection. For double screw connection as the steel thickness was increased as 8 mm, 12 mm, 16 mm, and 20 mm, the average capacity was increased to 0.79%, 4.91%, 2.15% accordingly.

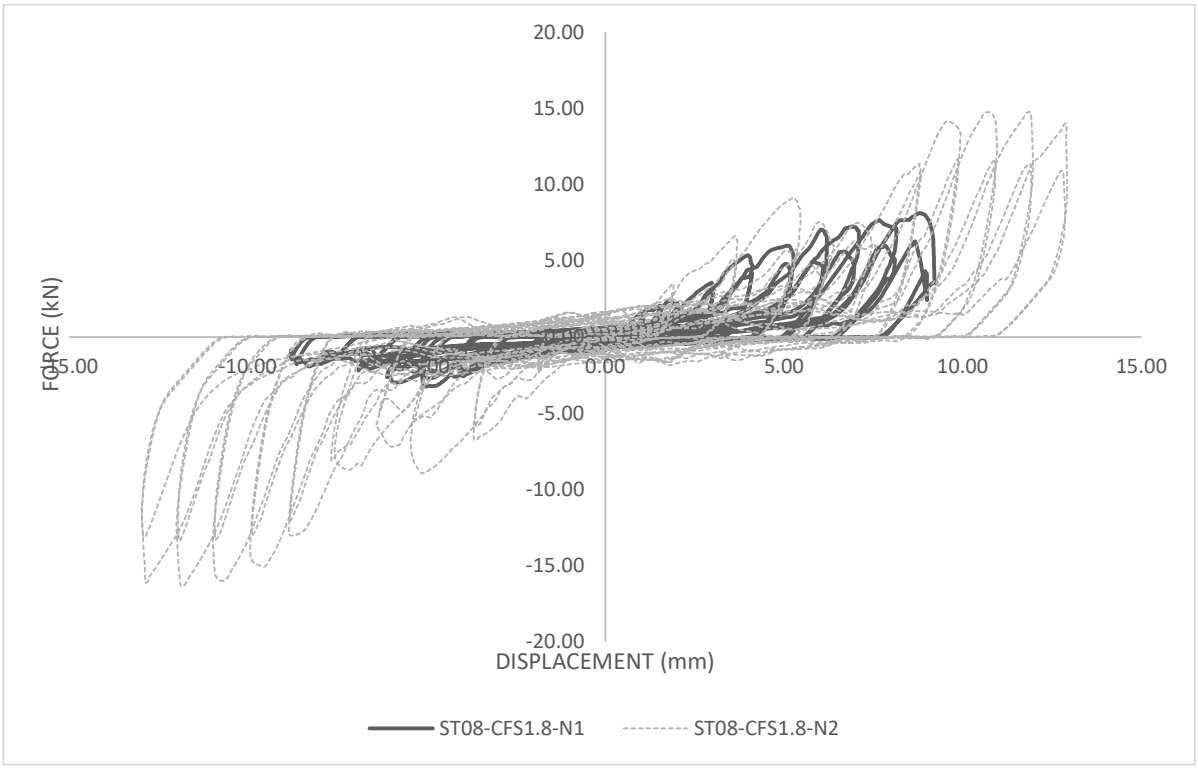

Fig. 30. The load-displacement curve for 8 mm steel plate

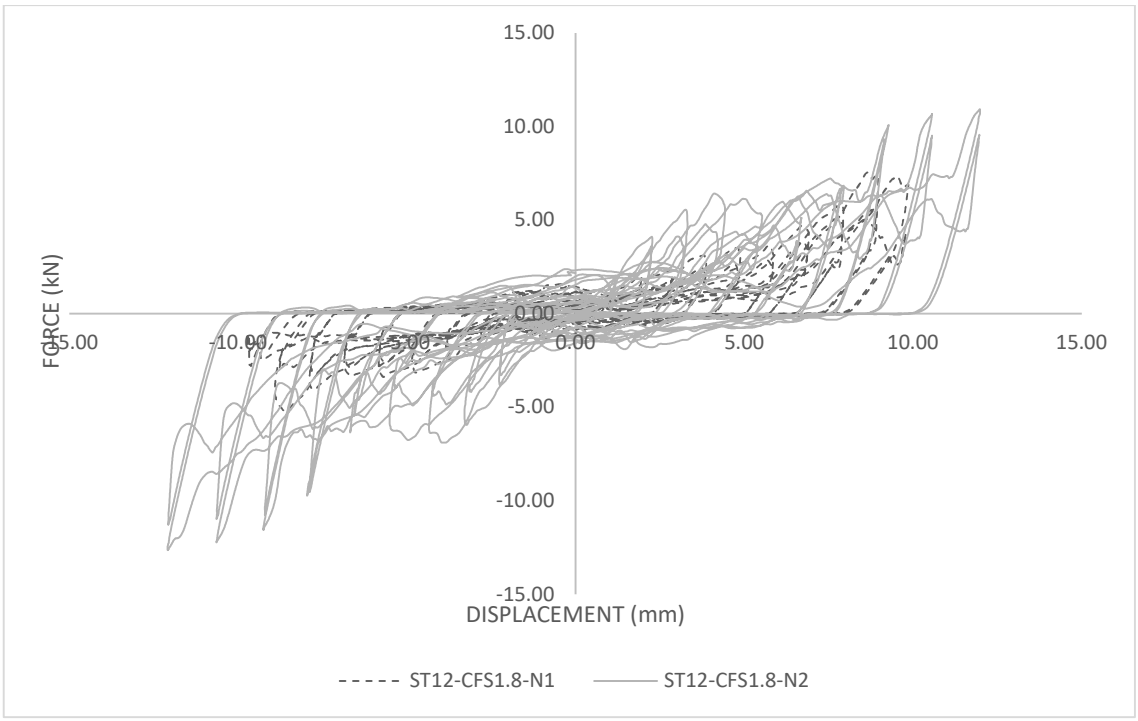

Fig. 31. The load-displacement curve for 12 mm steel plate

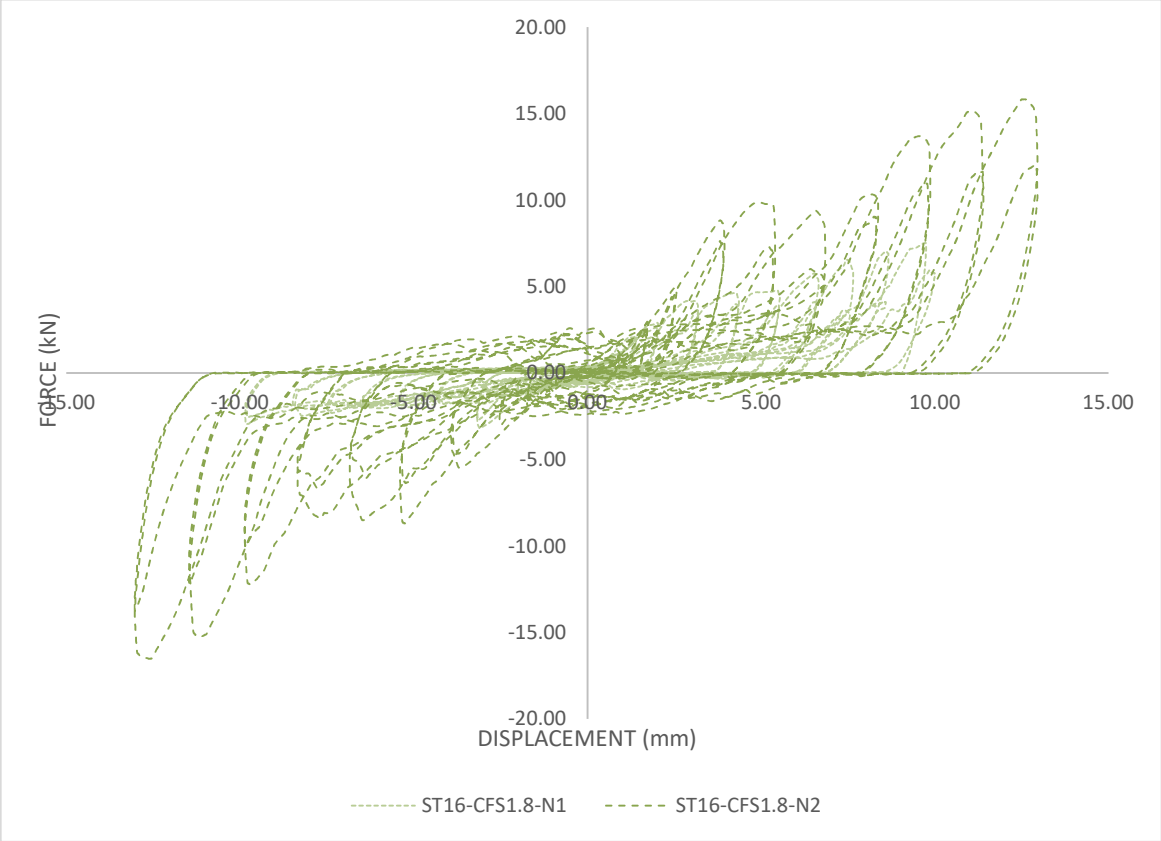

Fig. 32. The load-displacement curve for 16 mm steel plate

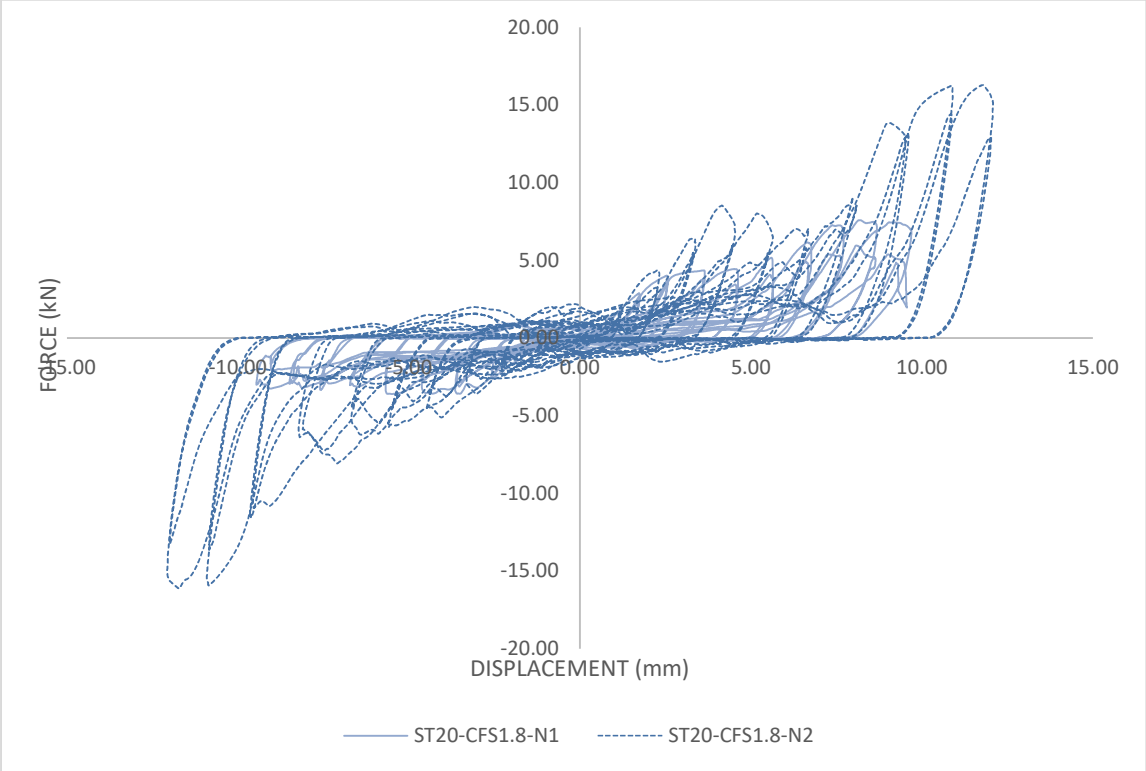

Fig. 33. The load-displacement curve for 20 mm steel plate

9. Conclusion

9.1. Conclusion

The experimental study presented in this paper aims to investigate the structural behaviour of self-drilling screw connections made for cold-formed and hot-rolled steel. Multiple types of material, shear, and cyclic tests were used to evaluate the composite connection's structural performance.

The seismic analysis of a light steel-framed building with a single and double shear steel fastener connection backbone and a fastener shear failure model is significantly advanced by this report. The models were developed using data from a comprehensive testing program that took into account both monotonic and cyclic loading. The main factor affecting the pre-peak connection stiffness and strength was the connected plies' bearing strengths.

The standard screw fastener connection is also updated and improved in this effort, and the test setup outlines a way to generalise cyclic loading. A non-contact computer vision measurement device that simply and precisely monitors relative displacement throughout the load deformation response is validated by a fastener protocol.

The screw connection's experimental studies produced a number of findings. An 8 mm steel to 1.8 mm CFS connection was the subject of a preliminary experimental research employing monotonic testing with a single screw connection. The findings indicate that the capacity stays constant, averaging 11.37 kN.

All of the screw specimens failed in both bearing and tear out failure, according to the experimental results of several screw connection tests, and the failure mode was significantly influenced by the thickness of the steel. For monotonic testing there was an average increase of 48.55% in capacity as the number of screws were increased from single screw to double screw connection. For cyclic testing there is an average increase of 56.77% in capacity as the number if screws were increased from single screw to double screw connection.

9.2. Limitation

These are the limitations of the current study.

- The research is confined to specific grades of steel and CFS.
- Due to the drilling capacity of the screw, the study was restricted to a single screw diameter.
- The codes do not provide sufficient information related to failure modes. Therefore, further research should be conducted to analyse using parameters like different grades of steel and CFS, and different screw arrangements for further evaluation of connection strength.

10.Acknowledgement

Firstly, I would like to express my deep gratitude to my first supervisor Dr Arthur Zhiyuan Fang, for his advice, assistance, guidance, and patience.

Also, I would like to express my sincere appreciation to Dr Krishanu Roy, and Professor James Lim for their expertise, thoughtful advice, and constant encouragement.

My best thanks to Jerry MA from Wurth for supplying all the Screws, structural steel sheets, CFS steel and tools for this research.

I want to thank my friends Shubham Tiwari, Kushal Ghosh, Gowrava Mohanswamy, Gagan Sengundham Dinesh, Vivekanandan Shivaji, Harsh Birwadkar, Puviyarasan Velayudham.

I want to express my gratitude to my family, my husband Dani Dominic, my father Antony A, and my mother Jancy Antony, and my brother Antony Mangalath for their support and motivation to complete this project.

Finally, I would like to thank the University of Waikato technicians Sophia Rodrigues, Jing Xu, Jonathan van Harselaar, Denis Jouan, Peter Higgins, Stephen Gwerder, and Bradley Scott for their help and assistance during laboratory testing.

11.Reference

Alireza Abaszadeh, Ali Mohammad Rousta, Ali Golsoorat Pahlaviani, & Peyman Beiranvand. (2021). Behavior of Connections in Cold-Formed Steel Frames under Cycling Loading. Practice Periodical on Structural Design and Construction, 26(2). https://doi.org/10.1061/(asce)sc.1943-5576.0000558

American Society for Testing and Materials, ASTM E8/E8M-21: Standard Test Methods for Tension Testing of Metallic Materials. 2021.

Ataei, A., Chiniforush, A. A., Bradford, M., & Valipour, H. (2019). Cyclic behaviour of bolt and screw shear connectors in steel-timber composite (STC) beams. Journal of Constructional Steel Research, 161, 328–340. https://doi.org/10.1016/j.jcsr.2019.05.048

Ballio, G., Calado, L., & Castiglioni, C. A. (1997). LOW CYCLE FATIGUE BEHAVIOUR OF STRUCTURAL STEEL MEMBERS AND CONNECTIONS. Fatigue & Fracture of Engineering Materials & Structures, 20(8), 1129–1146. https://doi.org/10.1111/j.1460-2695.1997.tb00318.x

Bellini, A., Benedetti, L., Pozza, L., & Mazzotti, C. (2020). Experimental characterization of monotonic and cyclic behavior of steel-to-CLT nailed joints strengthened with composite plies. Construction and Building Materials, 256, 119460. https://doi.org/10.1016/j.conbuildmat.2020.119460

Bernuzzi, C., Calado, L., & Castiglioni, C. A. (2000). Seismic behaviour of welded beam-to-columns joints: experimental and numerical analysis. 1–10.

Beutel, J., Thambiratnam, D., & Perera, N. (2001). Monotonic behaviour of composite column to beam connections. Engineering Structures, 23(9), 1152–1161. https://doi.org/10.1016/s0141-0296(01)00002-5

Beutel, J., Thambiratnam, D., & Perera, N. (2002). Cyclic behaviour of concrete filled steel tubular column to steel beam connections. Engineering Structures, 24(1), 29–38. https://doi.org/10.1016/s0141-0296(01)00083-9

Boadi-Danquah, E., Yount, T., Collins, W., & Fadden, M. (2021). Cyclic behavior of single shear steel-to-steel screws and powder-actuated fastener connections. Engineering Structures, 244, 112809–112809. https://doi.org/10.1016/j.engstruct.2021.112809

Calderoni, B., De Martino, A., Formisano, A., & Fiorino, L. (2009). Cold formed steel beams under monotonic and cyclic loading: Experimental investigation. Journal of Constructional Steel Research, 65(1), 219–227. https://doi.org/10.1016/j.jcsr.2008.07.014

Cao, J., Xiong, H., & Liu, Y. (2021). Experimental study and analytical model of bolted connections under monotonic loading. Construction and Building Materials, 270, 121380. https://doi.org/10.1016/j.conbuildmat.2020.121380

Chen, Z., Niu, X., Liu, J., & Khan, K. (2021). Experimental study of thin-walled steel-timber single-shear connection with a self-tapping screw. Structures, 34, 4389–4405. https://doi.org/10.1016/j.istruc.2021.10.028

Chui, Y. H., & Li, Y. (2005). Modeling Timber Moment Connection under Reversed Cyclic Loading. Journal of Structural Engineering, 131(11), 1757–1763. https://doi.org/10.1061/(asce)0733-9445(2005)131:11(1757)

Chung, K. F., & Ip, K. H. (2000). Finite element modeling of bolted connections between cold-formed steel strips and hot rolled steel plates under static shear loading. Engineering Structures, 22(10), 1271–1284. https://doi.org/10.1016/s0141-0296(99)00082-6

Closen, M. (2012). Self-tapping screw assemblies under monotonic and reverse cyclic load. https://doi.org/10.14288/1.0072901

Deng, E.-F., Zong, L., Ding, Y., Dai, X.-M., Lou, N., & Chen, Y. (2018). Monotonic and cyclic response of bolted connections with welded cover plate for modular steel construction. Engineering Structures, 167, 407–419. https://doi.org/10.1016/j.engstruct.2018.04.028

Fang, Z., Roy, K., Chen, B., Xie, Z., & Lim, J. B. (2021). Local and distortional buckling behaviour of aluminium alloy back-to-back channels with web holes under axial compression. Journal of Building Engineering, 47, 103837. https://doi.org/10.1016/j.jobe.2021.103837

Fang, Z., Roy, K., Chen, B., Xie, Z., Ingham, J., & Lim, J. B. (2022). Effect of the web hole size on the axial capacity of back-to-back aluminium alloy channel section columns. Engineering Structures, 260, 114238. https://doi.org/10.1016/j.engstruct.2022.114238

Fang, Z., Roy, K., Lakshmanan, D., Pranomrum, P., Li, F., Lau, H. H., & Lim, J. B. (2022). Structural behaviour of back-to-back cold-formed steel channel sections with web openings under axial compression at elevated temperatures. Journal of Building Engineering, 54, 104512. https://doi.org/10.1016/j.jobe.2022.104512

FEMA (2007). “FEMA 461 - Interim protocols for determining seismic performance characteristics of structural and nonstructural components through laboratory testing.” Federal Emergency Management Agency (FEMA), Document No. FEMA 461. Washington, D.C.

FEMA (2009). “FEMA P695 - Quantification of Building Seismic Performance Factors.” Federal Emergency

Management Agency (FEMA), Document No. FEMA 965. 2009, Washington, D.C.
Feng, R., Cai, Q., Ma, Y., & Yan, G. (2020). Shear analysis of self-drilling screw connections of CFS walls with steel sheathing. Journal of Constructional Steel Research, 167, 105842. https://doi.org/10.1016/j.jcsr.2019.105842
Fiorino, L., Della Corte, G., & Landolfo, R. (2007). Experimental tests on typical screw connections for cold-formed steel housing. Engineering Structures, 29(8), 1761–1773. https://doi.org/10.1016/j.engstruct.2006.09.006
Gavric, I., Fragiacomo, M., & Ceccotti, A. (2014). Cyclic behaviour of typical metal connectors for cross-laminated (CLT) structures. Materials and Structures, 48(6), 1841–1857. https://doi.org/10.1617/s11527-014-0278-7
He, J., Yoda, T., Takaku, H., Liu, Y., Chen, A., & Iura, M. (2010). Experimental and numerical study on cyclic behaviour of steel beam-to-column joints. International Journal of Steel Structures, 10(2), 131–146. https://doi.org/10.1007/bf03215825
Hossain, A., Popovski, M., & Tannert, T. (2018). Cross-laminated timber connections assembled with a combination of screws in withdrawal and screws in shear. Engineering Structures, 168, 1–11. https://doi.org/10.1016/j.engstruct.2018.04.052
Ibarra, L. F., Medina, R. A., & Krawinkler, H. (2005). Hysteretic models that incorporate strength and stiffness deterioration. Earthquake Engineering & Structural Dynamics, 34(12), 1489–1511. https://doi.org/10.1002/eqe.495
Iuorio, O., Macillo, V., Terracciano, M. T., Pali, T., Fiorino, L., & Landolfo, R. (2014). Seismic response of Cfs strap-braced stud walls: Experimental investigation. Thin-Walled Structures, 85, 466–480. https://doi.org/10.1016/j.tws.2014.09.008
Izzi, M., & Polastri, A. (2019). Low cycle ductile performance of screws used in timber structures. Construction and Building Materials, 217, 416–426. https://doi.org/10.1016/j.conbuildmat.2019.05.087
Izzi, M., Casagrande, D., Bezzi, S., Pasca, D., Follesa, M., & Tomasi, R. (2018). Seismic behaviour of Cross-Laminated Timber structures: A state-of-the-art review. Engineering Structures, 170, 42–52. https://doi.org/10.1016/j.engstruct.2018.05.060
Kishiki, S., Lee, D.-S., Yamada, S., Ishida, T., & Jiao, Y. (2019). Low-cycle fatigue performance assessment of current Japanese steel beam-to-column connections determined by ductile fracture. Engineering Structures, 182, 241–250. https://doi.org/10.1016/j.engstruct.2018.12.061
Latour, M., & Rizzano, G. (2014). Cyclic Behavior and Modeling of a Dissipative Connector for Cross-Laminated Timber Panel Buildings. Journal of Earthquake Engineering, 19(1), 137–171. https://doi.org/10.1080/13632469.2014.948645
Li, W., Ye, H., Liu, H., & Chen, B. (2022). Development and testing of demountable RC column-to-steel beam connections under cyclic loading. Soil Dynamics and Earthquake Engineering, 159, 107342–107342. https://doi.org/10.1016/j.soildyn.2022.107342
Ling, A., Hieng Ho Lau, Fang, Z., Roy, K., Raftery, G. M., & James B.P. Lim. (2023). Experimental studies of timber to cold-formed steel connections with self-drilling screws. Structures, 49, 492–507. https://doi.org/10.1016/j.istruc.2023.01.111
Mander, J. B., Freyan Panthaki, & Amarnath Kasalanati. (1994). Low-Cycle Fatigue Behavior of Reinforcing Steel. Journal of Materials in Civil Engineering, 6(4), 453–468. https://doi.org/10.1061/(asce)0899-1561(1994)6:4(453)
Mashaly, E., El-Heweity, M., Abou-Elfath, H., & Osman, M. (2011). Finite element analysis of beam-to-column joints in steel frames under cyclic loading. Alexandria Engineering Journal, 50(1), 91–104. https://doi.org/10.1016/j.aej.2011.01.012
Mroziński, S., Egner, H., & Piotrowski, M. (2019). Effects of fatigue testing on low-cycle properties of P91 steel. International Journal of Fatigue, 120, 65–72. https://doi.org/10.1016/j.ijfatigue.2018.11.001
Ng, A. L. Y., Lau, H. H., Fang, Z., Roy, K., Raftery, G. M., & Lim, J. B. (2023). Experimental studies of timber to cold-formed steel connections with self-drilling screws. Structures, 49, 492–507. https://doi.org/10.1016/j.istruc.2023.01.111
Popov, E. P., & Stephen, R. M. (1972). Cyclic loading of full-size steel connections.
Roy, K., Chen, B., Fang, Z., Uzzaman, A., & Lim, J. B. P. (2021). Axial capacity of Back-to-Back Built-Up aluminum alloy Channel section columns. Journal of Structural Engineering, 148(2). https://doi.org/10.1061/(asce)st.1943-541x.0003238
Roy, K., Lau, H. H., Fang, Z., Ahmed, A. M. M., & Lim, J. B. (2021). Axial capacity of back-to-back built-up cold-formed stainless steel unlipped channels-Numerical investigation and parametric study. Steel and Composite Structures, 40(5), 761. https://doi.org/10.12989/scs.2021.40.5.761
Roy, K., Lau, H. H., Fang, Z., Masood, R., Ting, T. C. H., Lim, J. B., & Lee, V. C. C. (2022). Effects of corrosion on the strength of self-drilling screw connections in cold-formed steel structures-experiments and finite element modeling. Structures, 36, 1080–1096. https://doi.org/10.1016/j.istruc.2021.12.052
Roy, K., Rezaeian, H., Lakshmanan, D., Fang, Z., Ananthi, G. B. G., & Lim, J. B. (2023). Structural behaviour of

cold-formed steel T-Stub connections with HRC and screws subjected to tension force. Engineering Structures, 283, 115922. https://doi.org/10.1016/j.engstruct.2023.115922
Schneider, J., Shen, Y., Stiemer, S. F., & Tesfamariam, S. (2015). Assessment and comparison of experimental and numerical model studies of cross-laminated timber mechanical connections under cyclic loading. Construction and Building Materials, 77, 197–212. https://doi.org/10.1016/j.conbuildmat.2014.12.029
Standards Australia & Standards New Zealand. (2018). AS/NZS 4600:2018 - Cold-formed steel structures. Standards Australia Limited & Standards New Zealand.
Standards New Zealand. (2021). NZS 3404:2021 - Steel structures standard. Standards New Zealand.
Tao, Fannie, A. Chatterjee, and C. D. Moen. "Monotonic and cyclic response of single shear cold-formed steel-to-steel and sheathing-to-steel connections." Virginia Tech Research Report No. CE/VPI-ST-16/01, Blacksburg, VA, USA. 2016.
Taylor, B., Barbosa, A. R., & Sinha, A. (2020). Cyclic performance of in-plane shear cross-laminated timber panel-to-panel surface spline connections. Engineering Structures, 218, 110726. https://doi.org/10.1016/j.engstruct.2020.110726
Vella, N., Gardner, L., & Buhagiar, S. (2020). Experimental analysis of cold-formed steel-to-timber connections with inclined screws. Structures, 24, 890–904. https://doi.org/10.1016/j.istruc.2020.02.009
Wurth New Zealand Ltd, Auckland New Zealand.
Y Oktavianus, Goldsworthy, H., & Gad, E. (2015). A study towards the development of a low damage moment-resisting connections using blind bolts, CFCHS columns and a replaceable energy dissipating device.
Zhou, H., Wang, Y., Yang, L., & Shi, Y. (2014). Seismic low-cycle fatigue evaluation of welded beam-to-column connections in steel moment frames through global–local analysis. International Journal of Fatigue, 64, 97–113. https://doi.org/10.1016/j.ijfatigue.2014.03.002

Appendix A Monotonic test for single screw connection

(a) Test setup

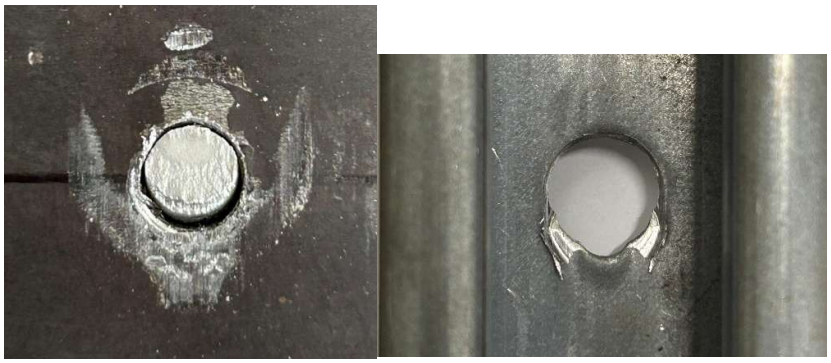

(b)Post-tested samples

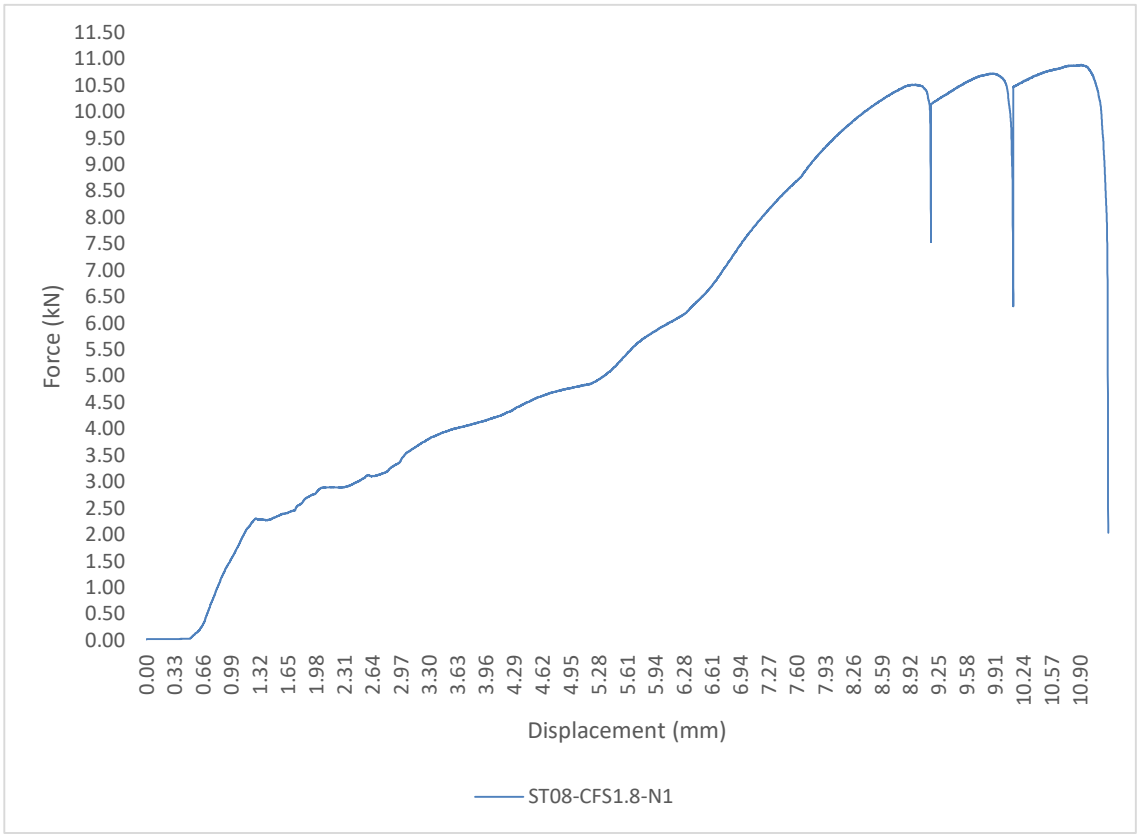

(c) Load v/s displacement curve for single screw of 8mm steel and 1.8mm CFS

Figure 34 Test result of ST08-CFS1.8-N1

(a) Test setup

(b)Post-tested samples

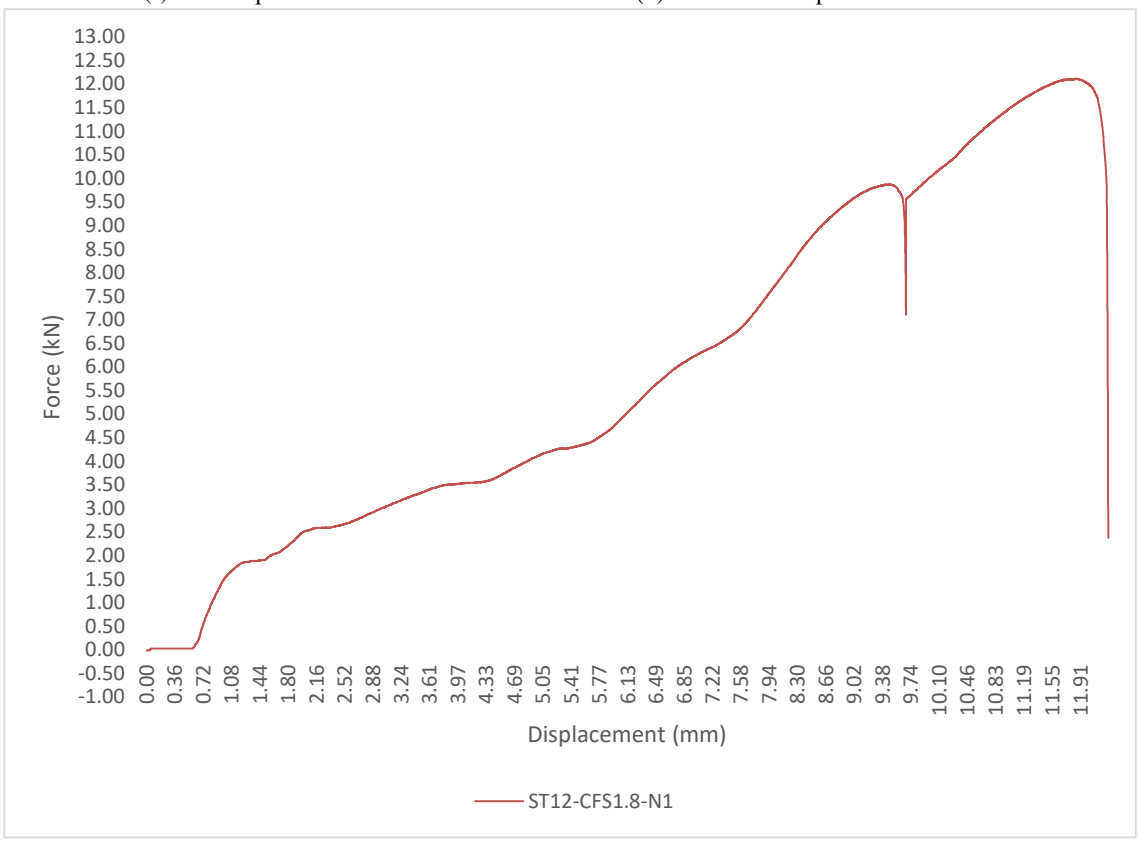

(c) Load v/s displacement curve for single screw of 12mm steel and 1.8mm CFS

Figure 35 Test result of ST12-CFS1.8-N1

(a) Test setup

(b)Post-tested samples

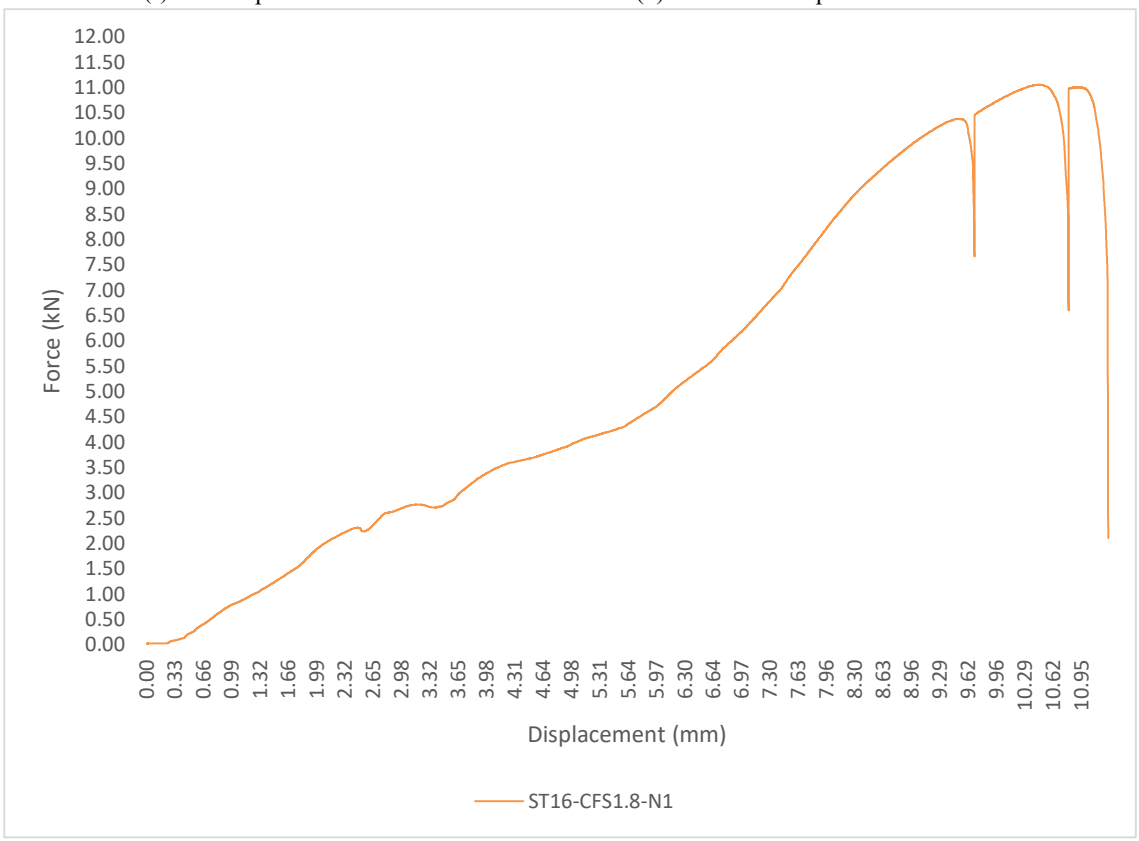

(c) Load v/s displacement curve for single screw of 16mm steel and 1.8mm CFS

Figure 36 Test result of ST16-CFS1.8-N1

(a) Test setup

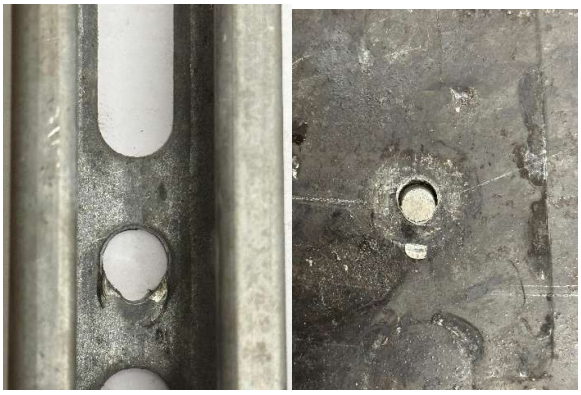

(b)Post-tested samples

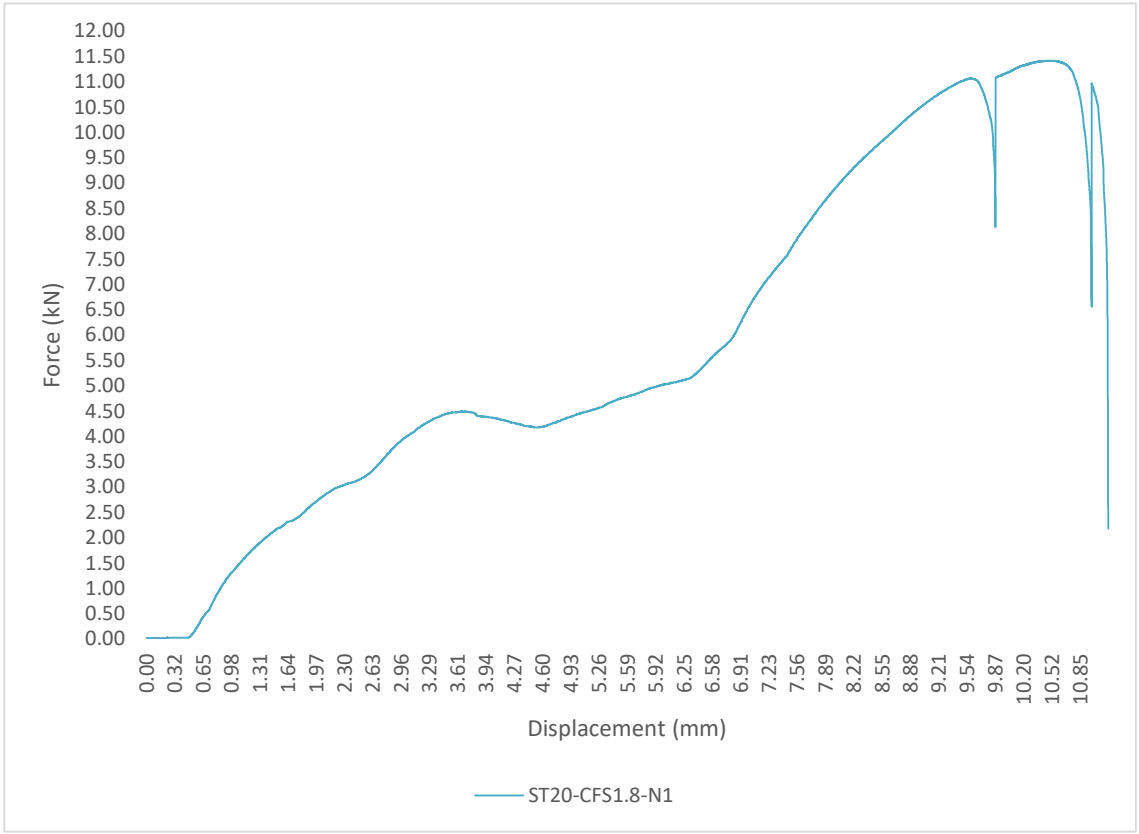

(c) Load v/s displacement curve for single screw of 20mm steel and 1.8mm CFS

Figure 37 Test result of ST20-CFS1.8-N1

Appendix B Monotonic test for double screw connection

(a) Test setup

(b)Post-tested samples

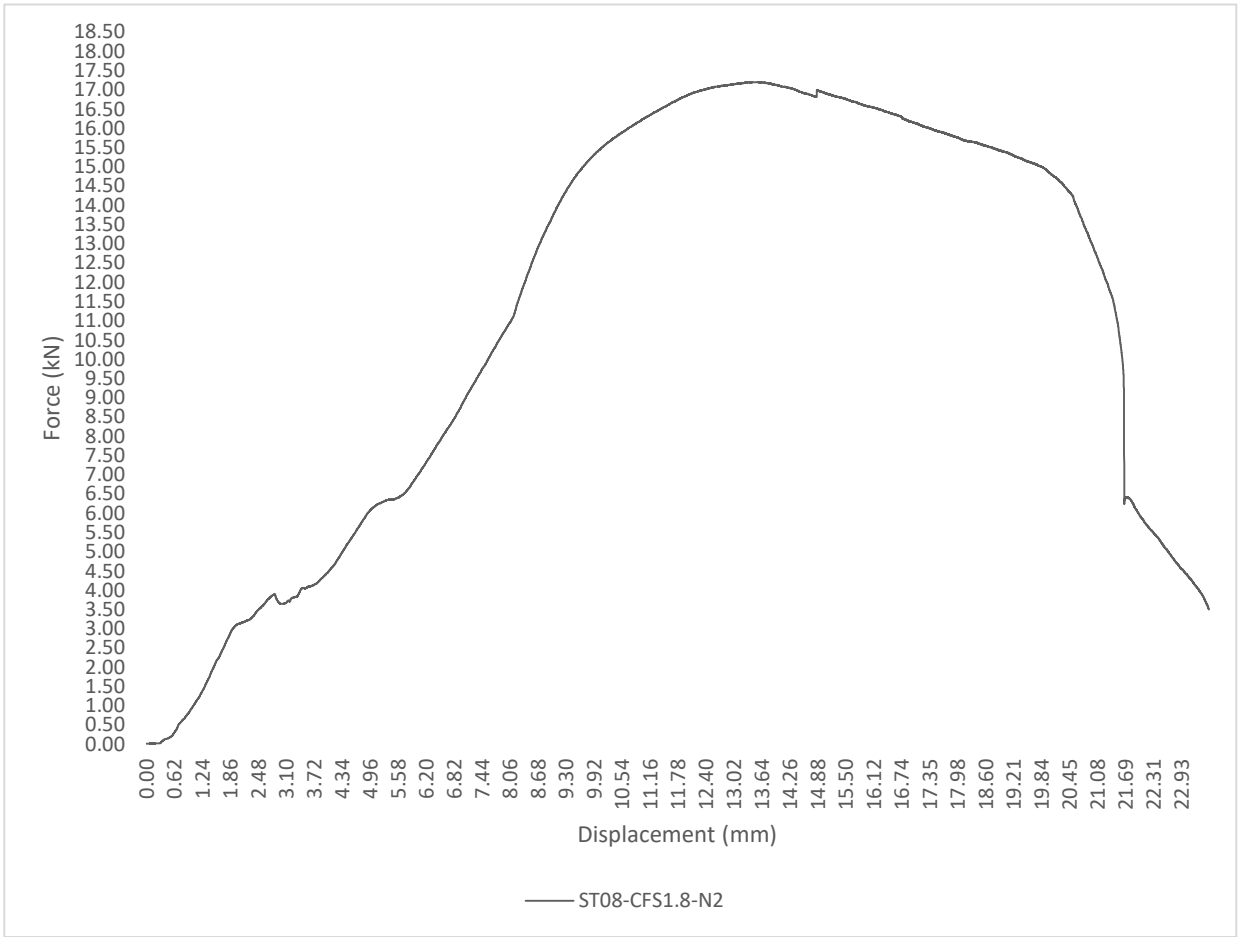

(c) Load v/s displacement curve for double screw of 8mm steel and 1.8mm CFS

Figure 38 Test result of ST08-CFS1.8-N2

(a) Test setup

(b)Post-tested samples

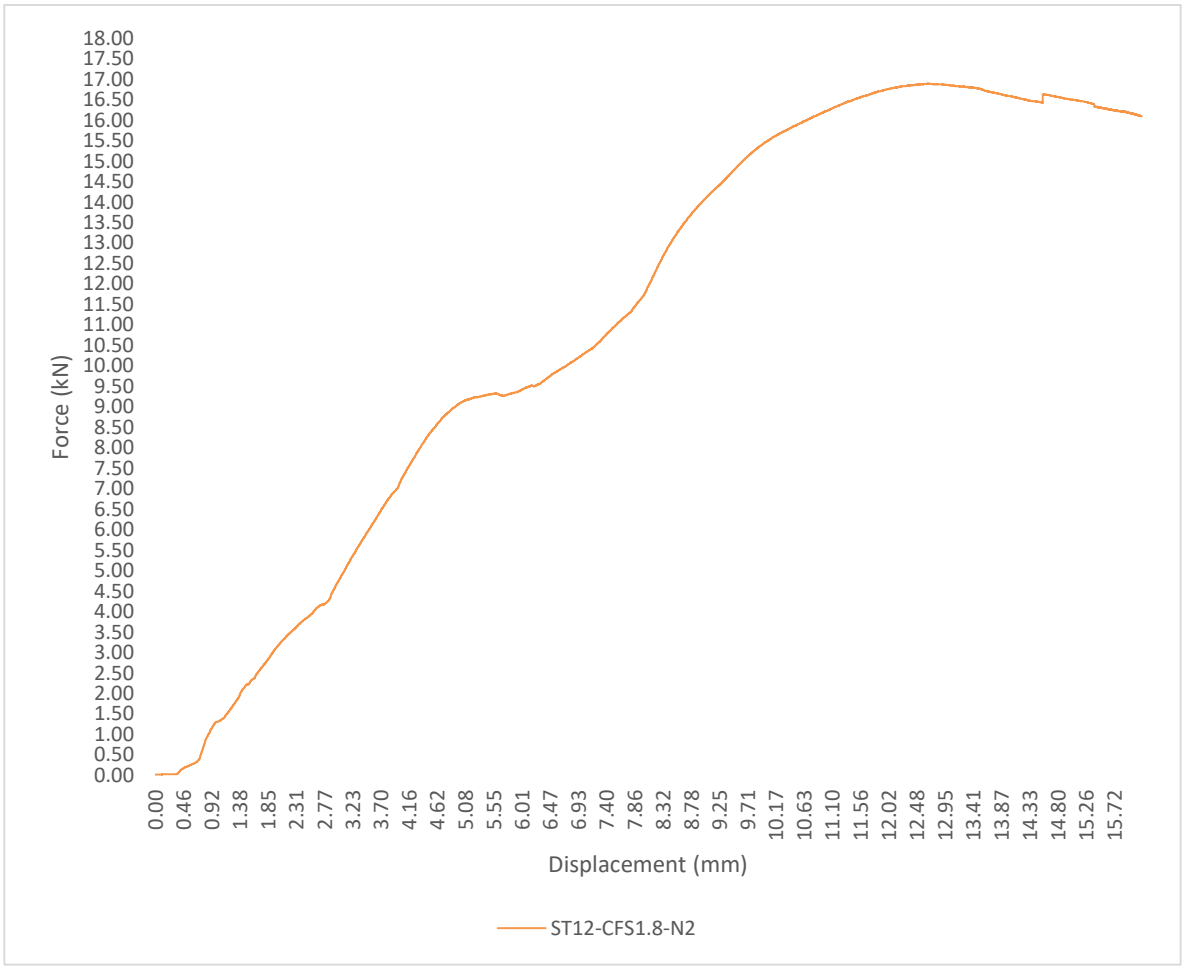

(c) Load v/s displacement curve for double screw of 12mm steel and 1.8mm CFS

Figure 39 Test result of ST12-CFS1.8-N2

(a) Test setup

(b)Post-tested samples

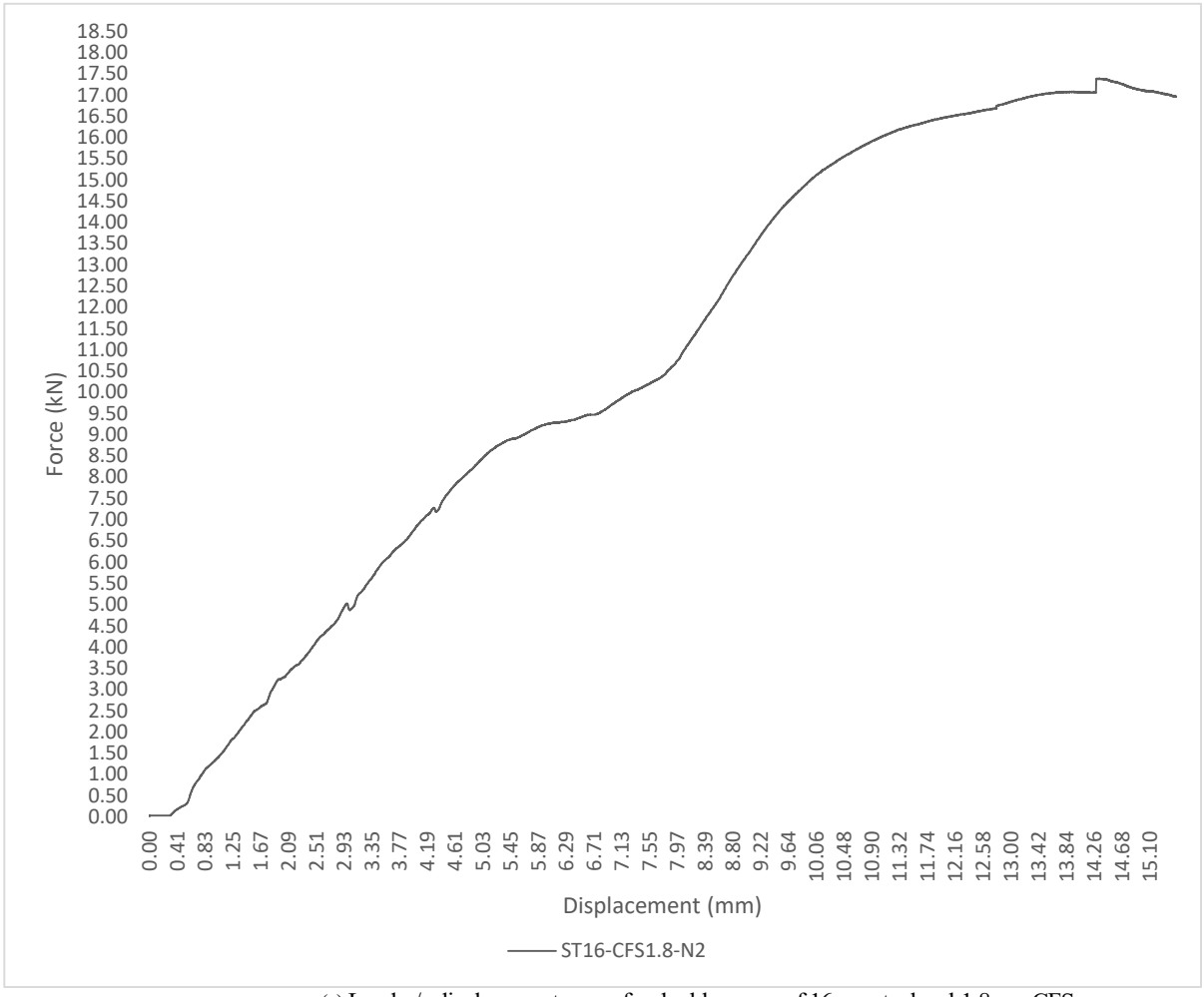

(c) Load v/s displacement curve for double screw of 16mm steel and 1.8mm CFS

Figure 40 Test result of ST16-CFS1.8-N2

(a) Test setup

(b)Post-tested samples

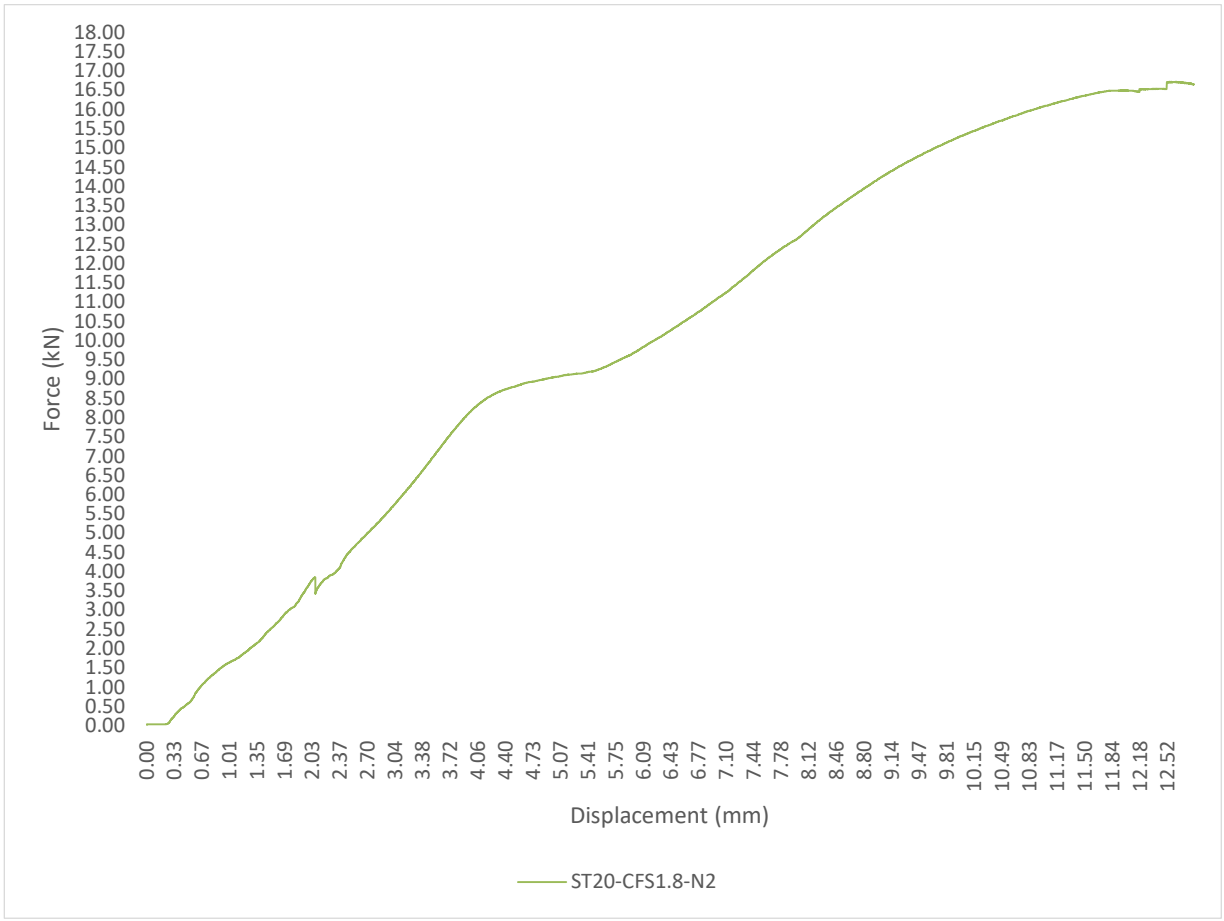

(c) Load v/s displacement curve for double screw of 20mm steel and 1.8mm CFS

Figure 41 Test result of ST20-CFS1.8-N2

Appendix C Cyclic test for single screw connection

(a)Post-tested samples

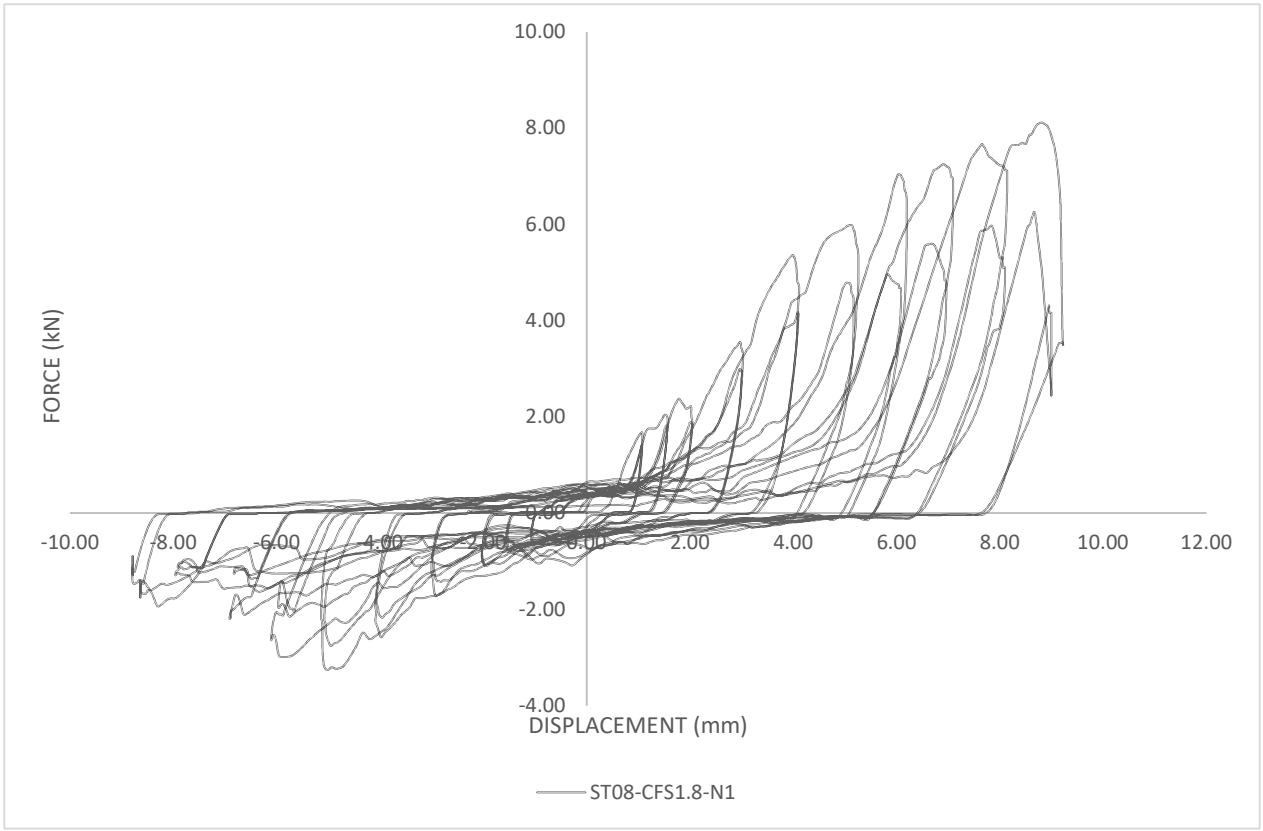

(b) Load v/s displacement curve for single screw of 8mm steel and 1.8mm CFS

Figure 42 Test result of ST08-CFS1.8-N1

(a)Post-tested samples

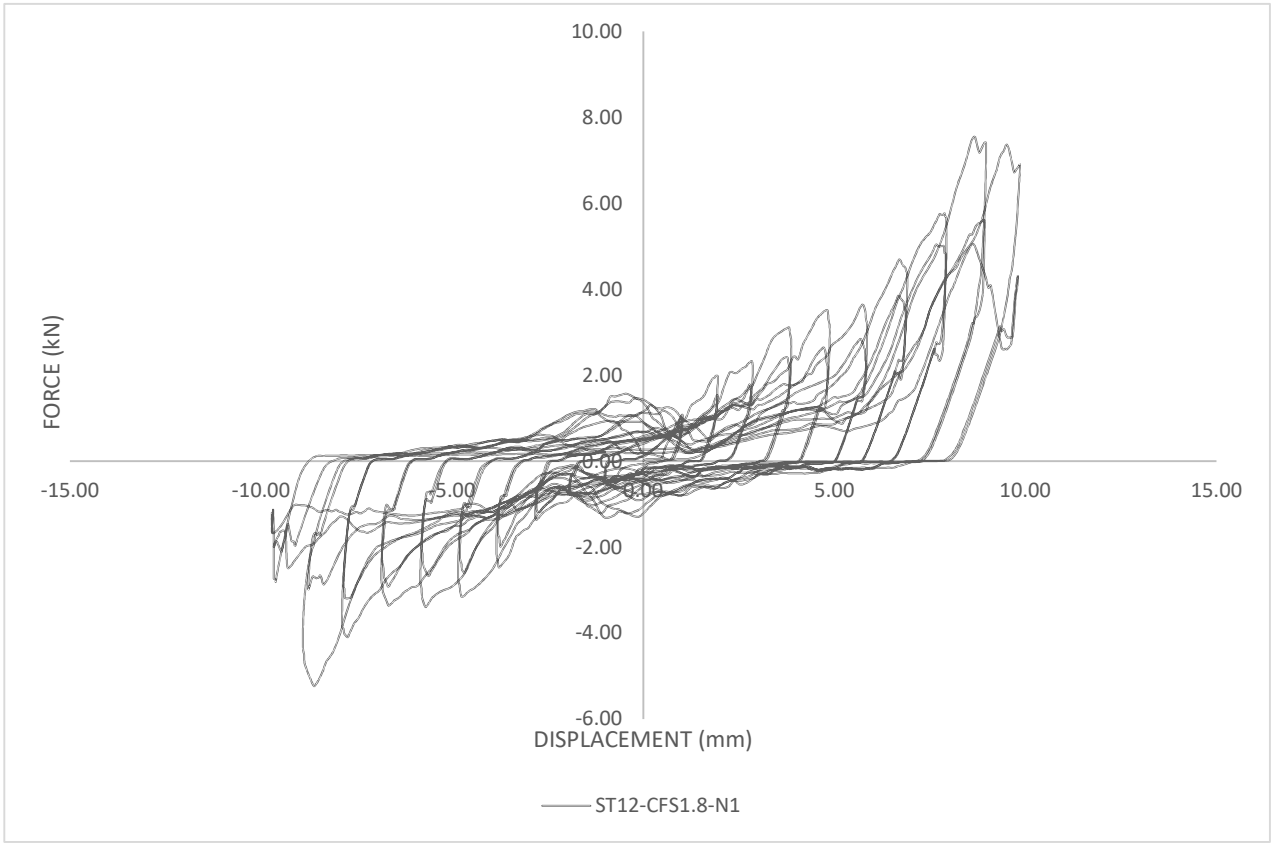

(b) Load v/s displacement curve for single screw of 12mm steel and 1.8mm CFS

Figure 43 Test result of ST12-CFS1.8-N1

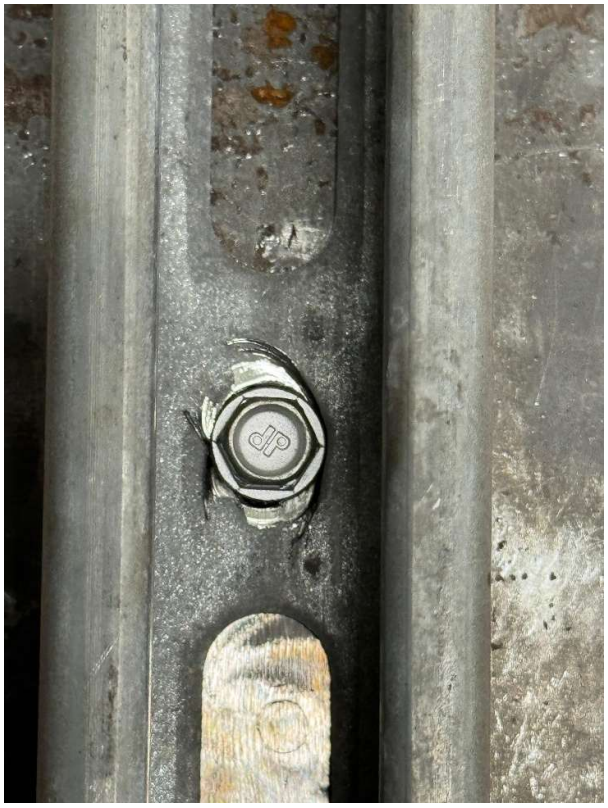

(a)Post-tested samples

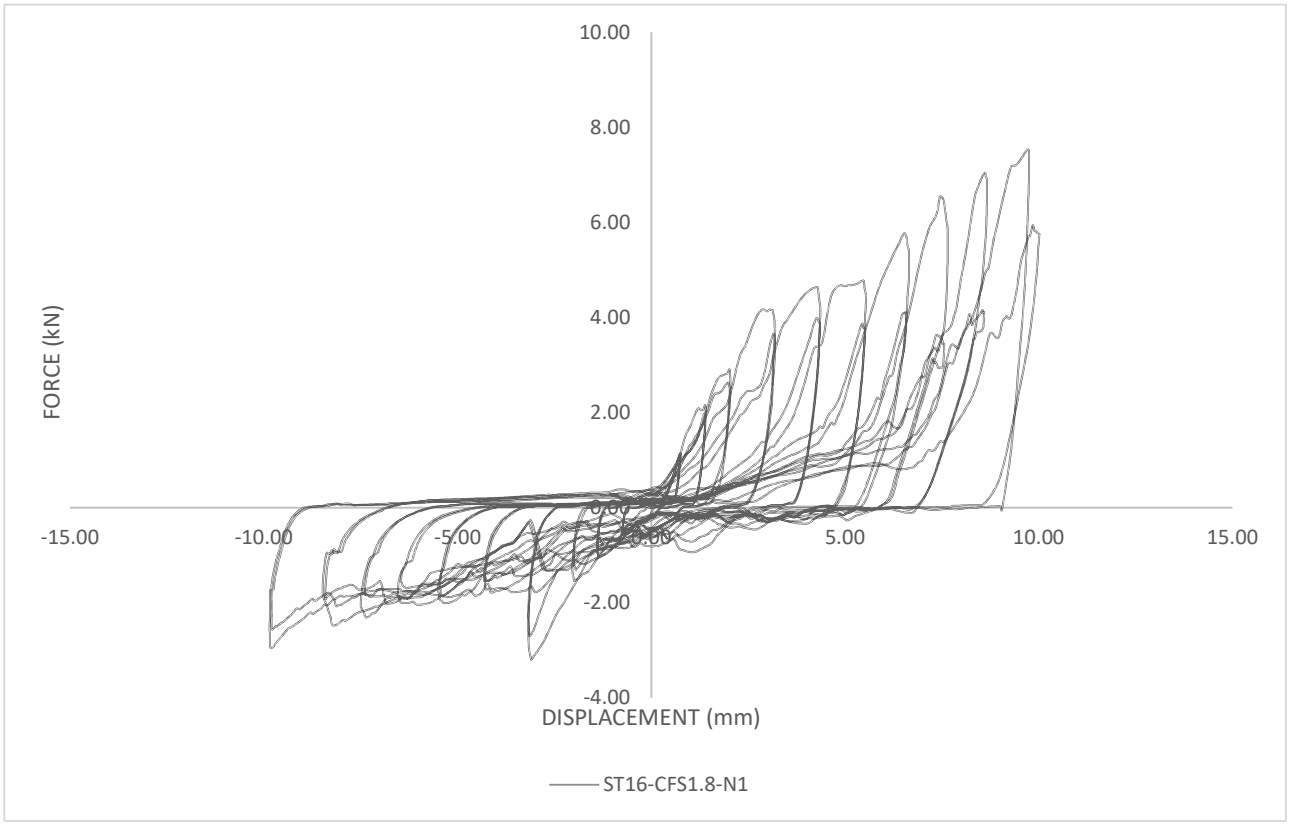

(b) Load v/s displacement curve for single screw of 16mm steel and 1.8mm CFS

Figure 44 Test result of ST16-CFS1.8-N1

(a)Post-tested samples

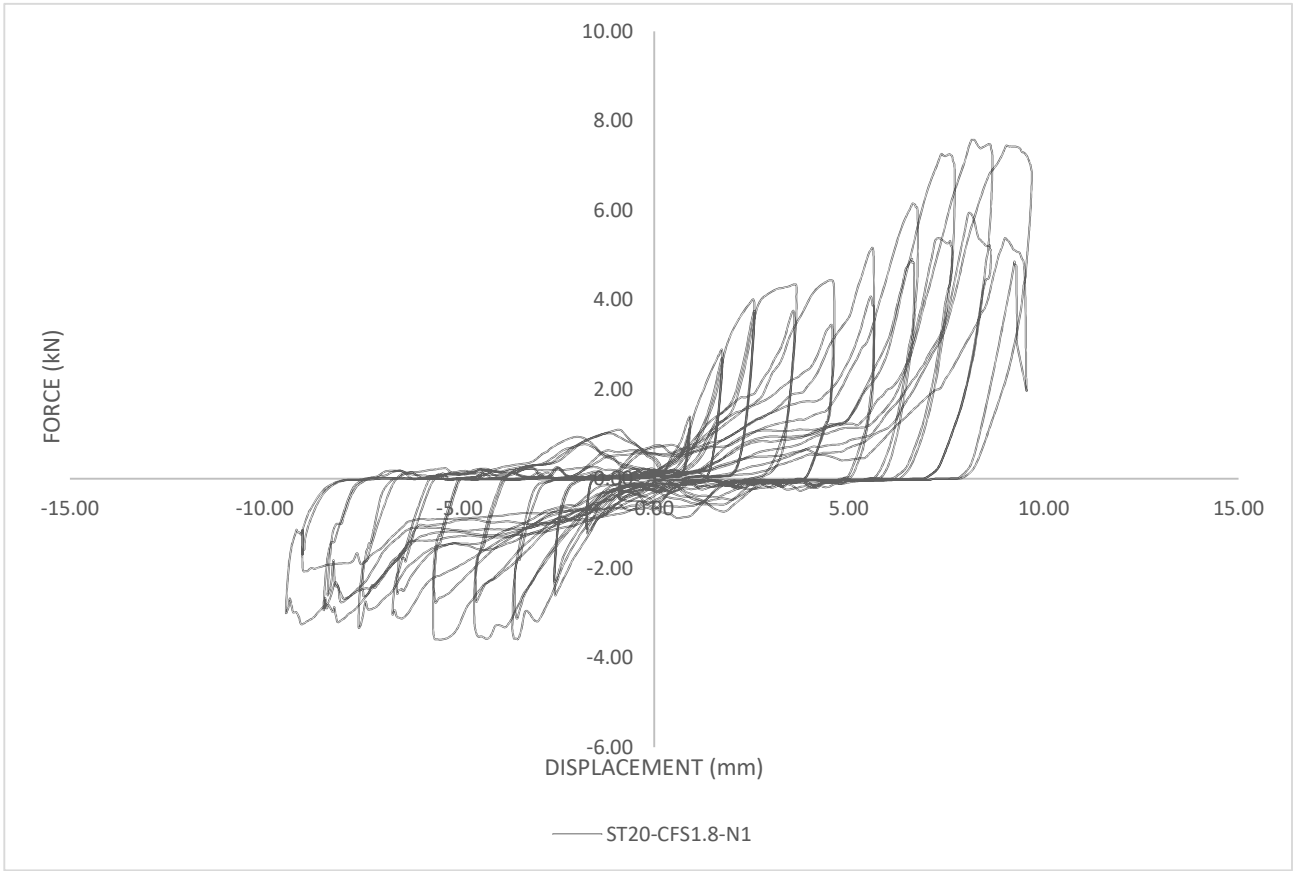

(b) Load v/s displacement curve for single screw of 20mm steel and 1.8mm CFS

Figure 45 Test result of ST20-CFS1.8-N1

Appendix D Cyclic test for double screw connection

(a)Post-tested samples

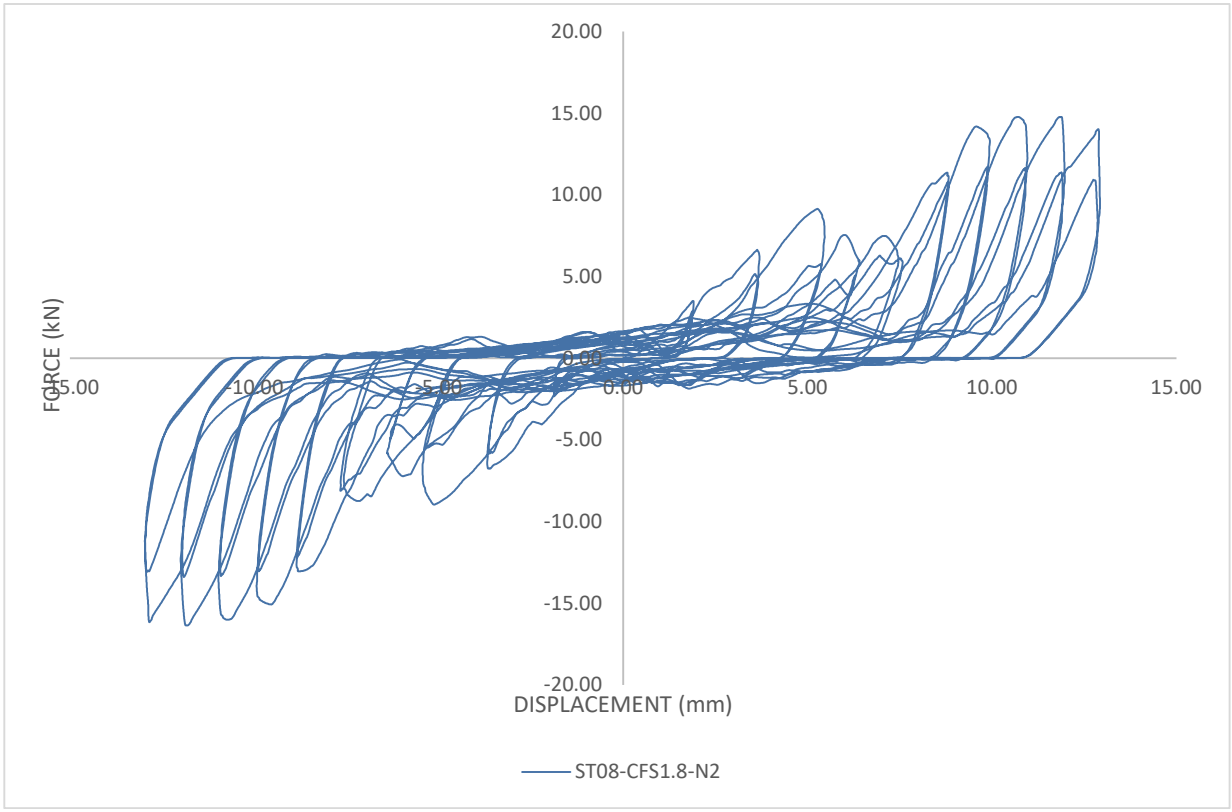

(b) Load v/s displacement curve for single screw of 8mm steel and 1.8mm CFS

Figure 46 Test result of ST08-CFS1.8-N2

(a)Post-tested samples

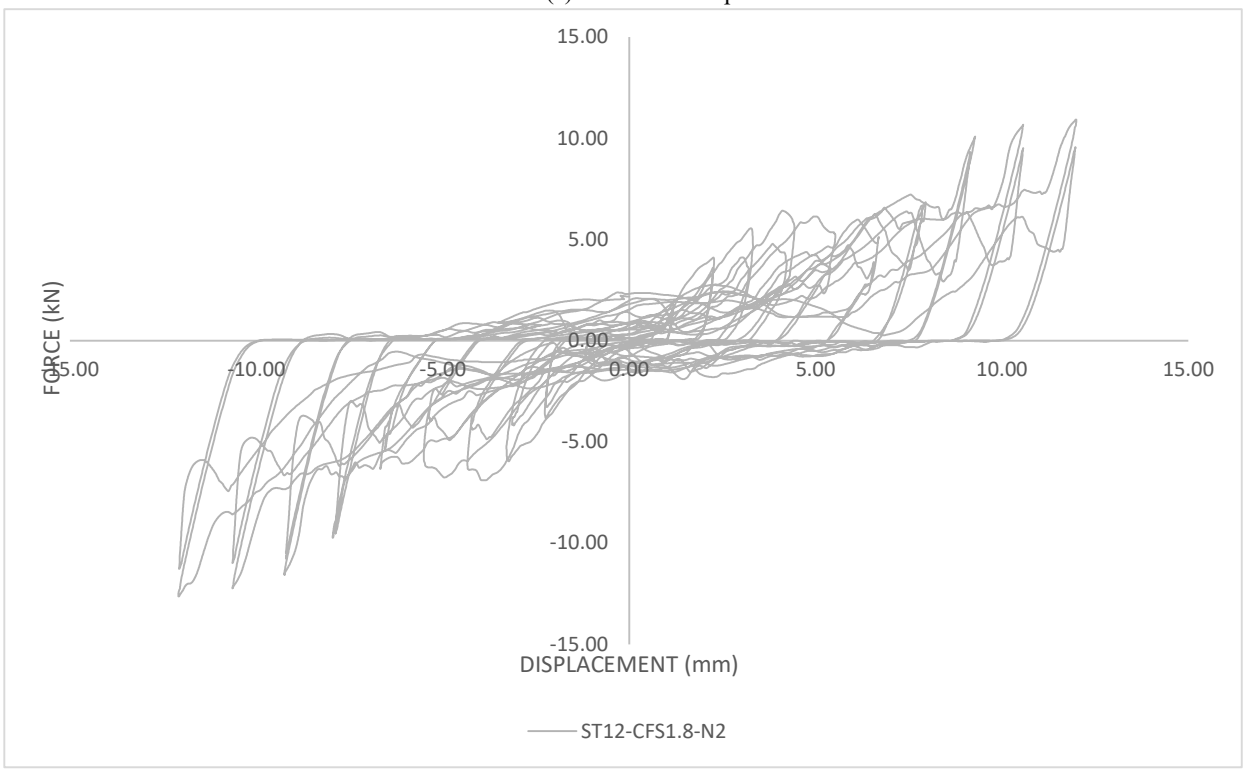

(b) Load v/s displacement curve for single screw of 12mm steel and 1.8mm CFS

Figure 47 Test result of ST12-CFS1.8-N2

(a)Post-tested samples

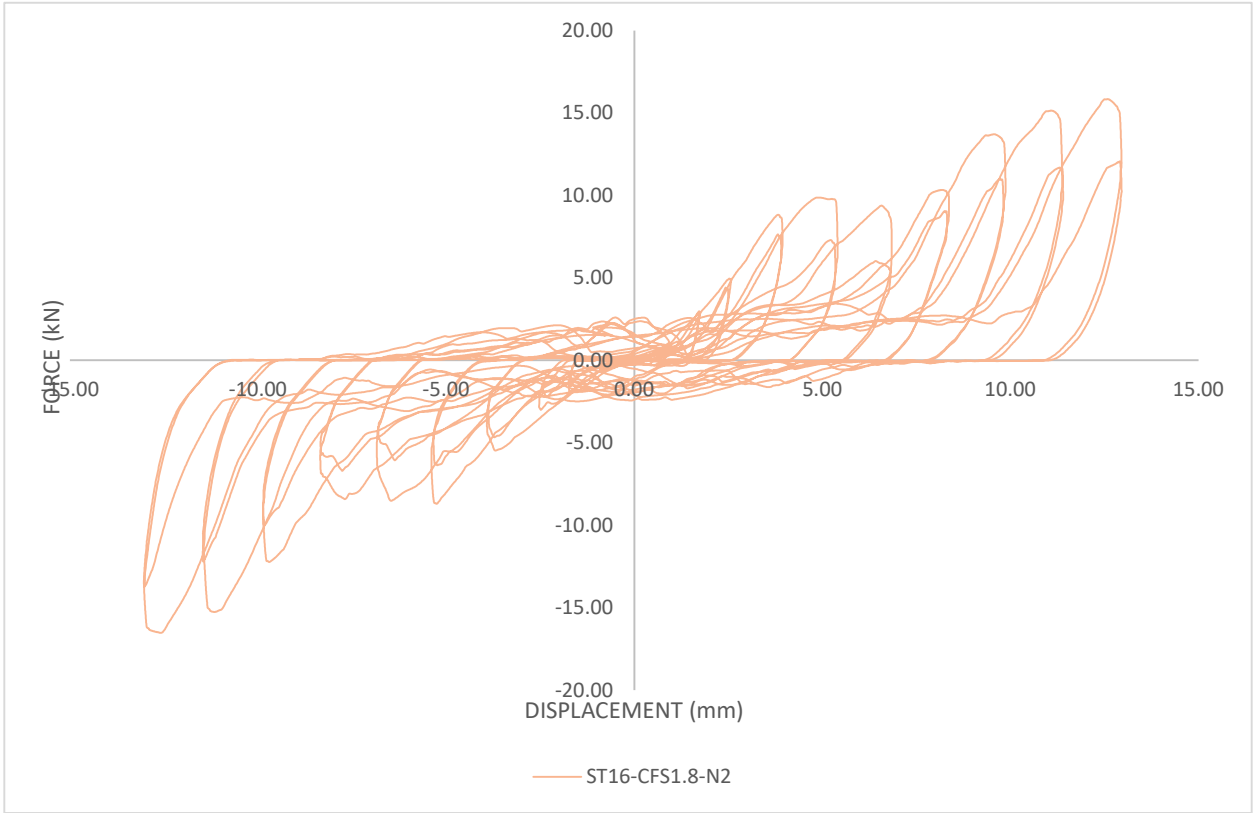

(b) Load v/s displacement curve for single screw of 16mm steel and 1.8mm CFS

Figure 48 Test result of ST16-CFS1.8-N2

(a)Post-tested samples

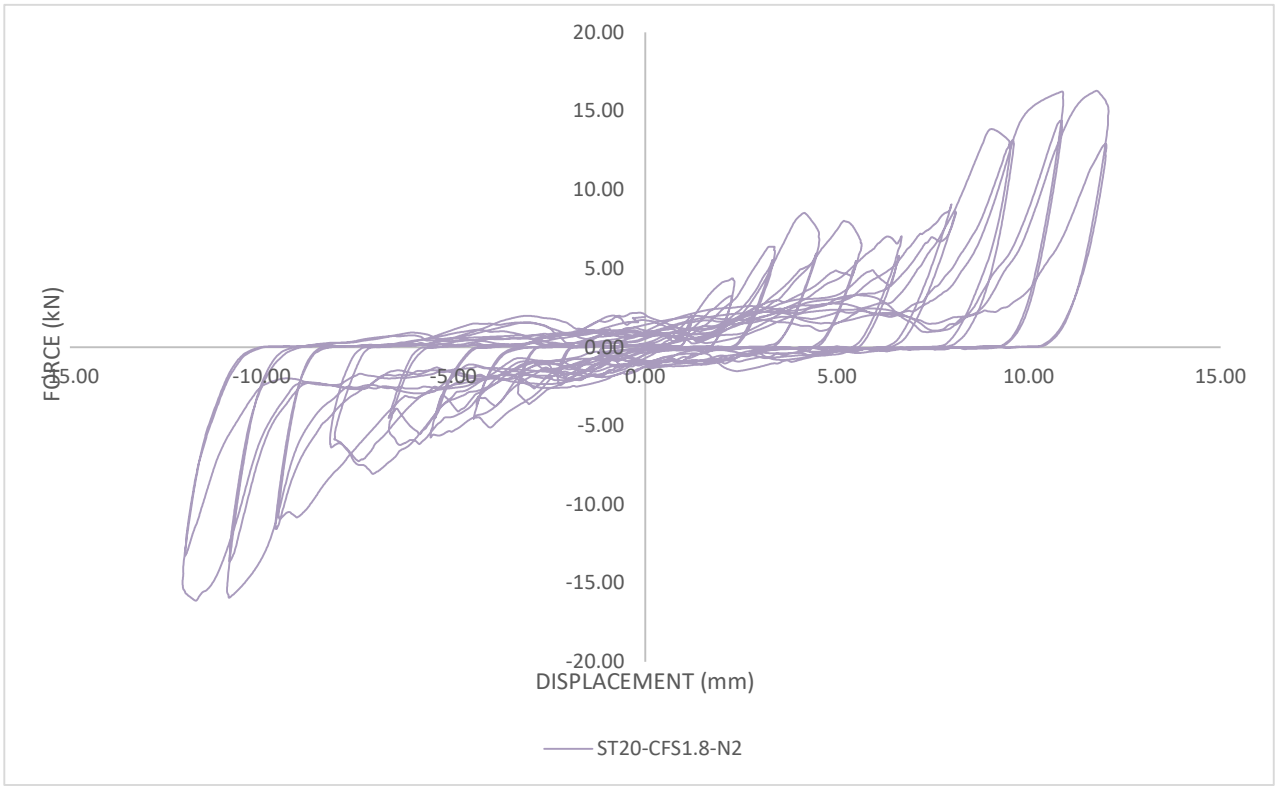

(b) Load v/s displacement curve for single screw of 20mm steel and 1.8mm CFS

Figure 49 Test result of ST20-CFS1.8-N2